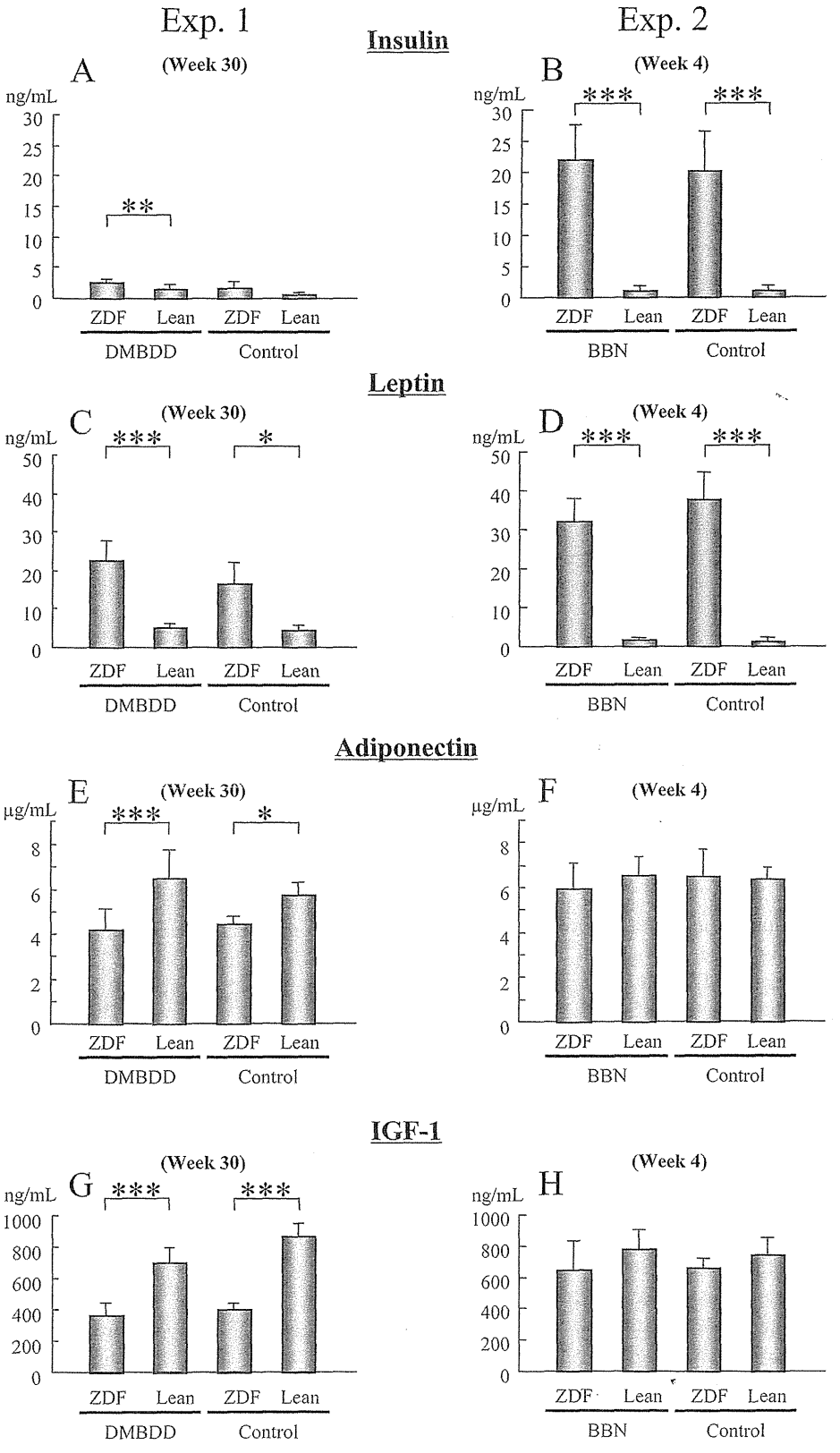

Fig. 4. Serum levels of insulin, leptin, adiponectin and IGF-1 in ZDF and Lean rats. Data from experiment 1 (A, C, E and G) and experiment 2 (B, D, F and H). Serum concentrations of insulin (A and B), leptin (C and D), adiponectin (E and F) and IGF-1 (G and H) were measured by ELISA. *, ** and ***: $P<0.05$, $P<0.001$ and $P<0.0001$, respectively, vs. Lean rats receiving the same treatment.

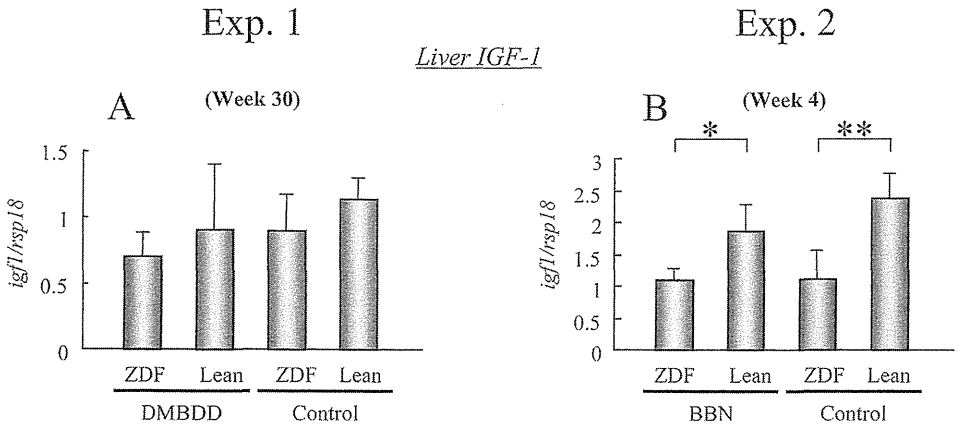

Fig. 5. IGF-1 mRNA expression in the liver. * and **: $P<0.05$ and $P<0.001$, respectively, vs. Lean rats receiving the same treatment.

vation of colon, pancreas, mammary, liver and urinary dder cancers[2,3]. To the best of our knowledge, this study vides the first experimental evidence for a relationship ween DM and urinary bladder cancer.

Several serum changes in T2DM patients have been gested to be responsible for the increased cancer risks, luding increases in insulin, IGF-1, leptin, TNFα and 6, as well as decreased adiponectin[15]. In the present dy, the serum insulin level was significantly higher in DMBDD-treated ZDF rats than in the DMBDD-treated n rats at week 30. It has been reported that hyperinsu-mia by injection of insulin enhanced the tumorigenesis azoxymethane-induced colon carcinogenesis in rats[16,17]. thermore, hyperinsulinemia is considered to promote cinogenesis not only directly but also indirectly by in-asing the synthesis of IGF-1[18]. Unexpectedly, the serum el of IGF-1 was significantly lower in the ZDF rats than he Lean rats irrespective of whether or not they received cinogen treatment at week 30, and there was no signifi-t difference at week 4 between the two strains of rats. In trast, the IGF-1 mRNA expression level in the liver, the or site of IGF-1 synthesis, was significantly lower in the F rats than in the Lean rats receiving the same treatment veek 4 but was not significant at week 30 between the two ins of rats. Further study examining the protein expres-n level of IGF-1 in the liver to explain this discrepancy is essary. Nevertheless, the changes of serum IGF-1 were related to the increased cancers of the urinary bladder, n and liver under the present conditions.

In recent studies, leptin, a hormone secreted by adi-ytes, was indicated to act as a mitogen and angiogenic or in addition to its neuroendocrine function[19]. Further-e, epidemiological studies have shown that an elevated el of serum leptin was associated with a high risk of rectal cancer in men[20] and breast cancer[21]. Meanwhile, nectin, which is also an adipocyte-secreted hormone, reported to have an antiproliferative effect[22]; thus, low nectin concentrations were associated with malignan-cies in the colon[23] or mammary gland[24]. In the present study, neither DMBDD initiation nor BBN treatment affected the serum levels of leptin or adiponectin in the ZDF and Lean rats; however, the serum level of leptin was significantly higher and the serum adiponectin level was significantly lower in the ZDF rats than in the Lean rats receiving the same treatment at week 30. Therefore, the elevation of leptin and decrease of adiponectin may represent a highly susceptible risk of carcinogenesis of the urinary bladder, colon and liver.

Recently, epidemiological studies have clearly indicated that individuals with diabetes have an increased risk of bladder cancer[3]; however, the mechanisms by which diabetes mellitus contributes to bladder carcinoma are not clear. In this study, both the incidence and multiplicity of bladder cancer were significantly increased in the DMBDD-treated ZDF rats compared with the treated Lean rats in the 30-week multiorgan carcinogenicity study. In the 4-week BBN bladder carcinogenicity study, the serum insulin level at week 4 was significantly increased in the treated and control ZDF rats compared with the Lean rats receiving the same treatment. Similarly, the serum leptin level in the ZDF rats was significantly increased compared with the Lean rats receiving the same treatment at week 4. On the other hand, no significant differences were apparent in the serum adiponectin level at week 4. Thus, changes of insulin and leptin, but not adiponectin levels, may be related to the high susceptibility of ZDF rats to bladder carcinogenesis from an early stage of carcinogenesis. Insulin and leptin have been reported to activate the PI3K signaling pathway[15], which is known to be associated with malignant behavior, including cell growth, proliferation and cell survival[25]. Furthermore, its activation of PI3K has been demonstrated to be responsible for carcinogenesis in regard to bladder, colon, liver and other cancers[26–29]. High mRNA expression levels of PI3K in the ZDF rats suggested that the PI3K pathway may be responsible for the high susceptibility to bladder carcinogenesis of rats with T2DM.

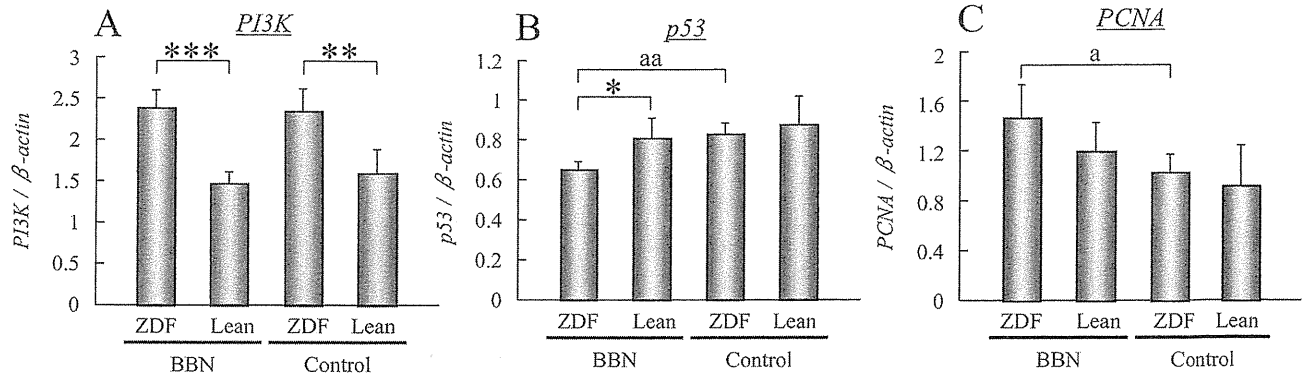

Fig. 6. PI3K, p53 and PCNA mRNA expression in the bladder epithelium of BBN-treated rats (experiment 2). *, ** and ***: $P<0.05$, $P<0.001$ and $P<0.0001$, respectively, vs. Lean rats receiving the same treatment. a and aa: $P<0.05$ and $P<0.001$, respectively, vs. control rats of the same genotype.

In addition, the decrease of p53 in obesity has been demonstrated to play an important role in obesity-associated cancers, such as breast and prostate cancer[30,31]. The low mRNA expression level of p53 in the BBN-treated ZDF rats compared with the BBN-treated Lean rats may be responsible, at least in part, for their high susceptibility to bladder carcinogenesis.

No increased risk of lung cancer in diabetes was found in a recent epidemiological study[32]. With regard to the relationship between diabetes and thyroid cancer risk, there is no report available in the published literature. The findings of the present study that the incidences and multiplicities of lung tumors and thyroid follicular carcinoma were significantly decreased in the DMBDD-treated ZDF rats compared with the DMBDD-initiated Lean group indicate a low susceptibility of ZDF rats to lung and thyroid carcinogenesis in this model. However, the mechanism by which T2DM affects lung and thyroid carcinogenesis and whether these findings are relevant to human lung and thyroid cancers are not currently clear.

In conclusion, our results demonstrated that urinary bladder, colon and liver carcinogenesis are enhanced in ZDF type 2 diabetes rats. The possible mechanisms are related to increased serum levels of insulin and leptin and a decreased serum level of adiponectin. Furthermore, the high susceptibility to bladder carcinogenesis in T2DM might be a consequence of PI3K pathway activation and decreased p53 expression. Further studies to analyze the mechanisms underlying the high susceptibility of T2DM rats to colon and liver carcinogenesis are necessary.

Acknowledgments: We gratefully acknowledge the expert technical assistance of Kaori Toma, Rie Onodera and Azusa Inagaki and the assistance of Yukiko Iura in preparation of this manuscript. This research was supported in part by a Health and Labour Sciences Research Grant from the Ministry of Health, Labour and Welfare of Japan.

References

1. Kasper DL, Brouwaid E, Fauci AS, Hauser SL, Longo DL, and Jameson JL. HARRISON'S PRINCIPLES OF Internal Medicine, Vol. 2005.
2. Nicolucci A. Epidemiological aspects of neoplasms in diabetes. Acta Diabetol. **47**: 87–95. 2010.
3. Larsson SC, Orsini N, Brismar K, and Wolk A. Diabetes mellitus and risk of bladder cancer: a meta-analysis. Diabetologia. **49**: 2819–2823. 2006.
4. Terai K, Sakamoto K, Goto M, Matsuda M, Kasamaki S, Shinmura K, Takita N, and Kamano T. Greater development of 1,2-dimethylhydrazine-induced colon cancer in a rat model of type 2 diabetes mellitus. J Int Med Res. **34**: 385–389. 2006.
5. Yoshizawa N, Yamaguchi H, Yamamoto M, Shimizu N, Furihata C, Tatematsu M, Seto Y, and Kaminishi M. Gastric carcinogenesis by N-Methyl-N-nitrosourea is enhanced in db/db diabetic mice. Cancer Sci. **100**: 1180–1185. 2009.
6. Cocca C, Gutierrez A, Nunez M, Croci M, Martin G, Cricco G, Rivera E, and Bergoc R. Suppression of mammary gland tumorigenesis in diabetic rats. Cancer Detect Prev. **27**: 37–46. 2003.
7. Giovannucci E. Insulin and colon cancer. Cancer Causes Control. **6**: 164–179. 1995.
8. Clark JB, Palmer CJ, and Shaw WN. The diabetic Zucker fatty rat. Proc Soc Exp Biol Med. **173**: 68–75. 1983.
9. Friedman JE, de Vente JE, Peterson RG, and Dohm GL. Altered expression of muscle glucose transporter GLUT-4 in diabetic fatty Zucker rats (ZDF/Drt-fa). Am J Physiol. **261**: E782–E788. 1991.
10. Sturis J, Pugh WL, Tang J, Ostrega DM, Polonsky JS, and Polonsky KS. Alterations in pulsatile insulin secretion in the Zucker diabetic fatty rat. Am J Physiol. **267**: E250–E259. 1994.
11. Fukushima S, Hagiwara A, Hirose M, Yamaguchi S, Tiwawech D, and Ito N. Modifying effects of various chemicals on preneoplastic and neoplastic lesion development in

a wide-spectrum organ carcinogenesis model using F344 rats. Jpn J Cancer Res. **82**: 642–649. 1991.
12. Doi K, Wanibuchi H, Salim EI, Shen J, Wei M, Mitsuhashi M, Kudoh S, Hirata K, and Fukushima S. Revised rat multi-organ carcinogenesis bioassay for whole-body detection of chemopreventive agents: modifying potential of S-methylcysteine. Cancer Lett. **206**: 15–26. 2004.
13. Wei M, Arnold L, Cano M, and Cohen SM. Effects of co-administration of antioxidants and arsenicals on the rat urinary bladder epithelium. Toxicol Sci. **83**: 237–245. 2005.
14. Wei M, Hamoud AS, Yamaguchi T, Kakehashi A, Morimura K, Doi K, Kushida M, Kitano M, Wanibuchi H, and Fukushima S. Potassium bromate enhances N-ethyl-N-hydroxyethylnitrosamine-induced kidney carcinogenesis only at high doses in Wistar rats: indication of the existence of an enhancement threshold. Toxicol Pathol. **37**: 983–991. 2009.
15. Huang XF, and Chen JZ. Obesity, the PI3K/Akt signal pathway and colon cancer. Obes Rev. **10**: 610–616. 2009.
16. Corpet DE, Jacquinet C, Peiffer G, and Tache S. Insulin injections promote the growth of aberrant crypt foci in the colon of rats. Nutr Cancer. **27**: 316–320. 1997.
17. Tran TT, Medline A, and Bruce WR. Insulin promotion of colon tumors in rats. Cancer Epidemiol Biomarkers Prev. **5**: 1013–1015. 1996.
18. Boni-Schnetzler M, Schmid C, Meier PJ, and Froesch ER. Insulin regulates insulin-like growth factor I mRNA in rat hepatocytes. Am J Physiol. **260**: E846–E851. 1991.
19. Garofalo C, and Surmacz E. Leptin and cancer. J Cell Physiol. **207**: 12–22. 2006.
20. Stattin P, Palmqvist R, Soderberg S, Biessy C, Ardnor B, Hallmans G, Kaaks R, and Olsson T. Plasma leptin and colorectal cancer risk: a prospective study in Northern Sweden. Oncol Rep. **10**: 2015–2021. 2003.
21. Han C, Zhang HT, Du L, Liu X, Jing J, Zhao X, Yang X, and Tian B. Serum levels of leptin, insulin, and lipids in relation to breast cancer in china. Endocrine. **26**: 19–24. 2005.
22. Barb D, Williams CJ, Neuwirth AK, and Mantzoros CS. Adiponectin in relation to malignancies: a review of existing basic research and clinical evidence. Am J Clin Nutr. **86**: s858–s866. 2007.
23. Wei EK, Giovannucci E, Fuchs CS, Willett WC, and Mantzoros CS. Low plasma adiponectin levels and risk of colorectal cancer in men: a prospective study. J Natl Cancer Inst. **97**: 1688–1694. 2005.
24. Tworoger SS, Eliassen AH, Kelesidis T, Colditz GA, Willett WC, Mantzoros CS, and Hankinson SE. Plasma adiponectin concentrations and risk of incident breast cancer. J Clin Endocrinol Metab. **92**: 1510–1516. 2007.
25. Cantley LC. The phosphoinositide 3-kinase pathway. Science. **296**: 1655–1657. 2002.
26. Knowles MA, Platt FM, Ross RL, and Hurst CD. Phosphatidylinositol 3-kinase (PI3K) pathway activation in bladder cancer. Cancer Metastasis Rev. **28**: 305–316. 2009.
27. Philp AJ, Campbell IG, Leet C, Vincan E, Rockman SP, Whitehead RH, Thomas RJ, and Phillips WA. The phosphatidylinositol 3'-kinase p85alpha gene is an oncogene in human ovarian and colon tumors. Cancer Res. **61**: 7426–7429. 2001.
28. Yeh KT, Chang JG, Chen YJ, Chen ST, Yu SY, Shih MC, Perng LI, Wang JC, Tsai M, and Chang CP. Mutation analysis of the putative tumor suppressor gene PTEN/MMAC1 in hepatocellular carcinoma. Cancer Invest. **18**: 123–129. 2000.
29. Vivanco I, and Sawyers CL. The phosphatidylinositol 3-kinase AKT pathway in human cancer. Nat Rev Cancer. **2**: 489–501. 2002.
30. Chen C, Chang YC, Liu CL, Chang KJ, and Guo IC. Leptin-induced growth of human ZR-75–1 breast cancer cells is associated with up-regulation of cyclin D1 and c-Myc and down-regulation of tumor suppressor p53 and p21WAF1/CIP1. Breast Cancer Res Treat. **98**: 121–132. 2006.
31. Mistry T, Digby JE, Desai KM, and Randeva HS. Leptin and adiponectin interact in the regulation of prostate cancer cell growth via modulation of p53 and bcl-2 expression. BJU Int. **101**: 1317–1322. 2008.
32. Hall GC, Roberts CM, Boulis M, Mo J, and MacRae KD. Diabetes and the risk of lung cancer. Diabetes Care. **28**: 590–594. 2005.

Hindawi Publishing Corporation
Experimental Diabetes Research
Volume 2011, Article ID 979354, 11 pages
doi:10.1155/2011/979354

Research Article

Targeted Proteomics of Isolated Glomeruli from the Kidneys of Diabetic Rats: Sorbin and SH3 Domain Containing 2 Is a Novel Protein Associated with Diabetic Nephropathy

Shinya Nakatani,[1,2] Anna Kakehashi,[1] Eiji Ishimura,[2] Shotaro Yamano,[1] Katsuhito Mori,[2] Min Wei,[1] Masaaki Inaba,[2] and Hideki Wanibuchi[1]

[1] *Department of Pathology, Osaka City University Graduate School of Medicine, 1-4-3 Asahi-machi, Abeno-ku, Osaka 545-8585, Japan*
[2] *Departments of Metabolism, Endocrinology, Molecular Medicine and Nephrology, Osaka City University Graduate School of Medicine, 1-4-3 Asahi-machi, Abeno-ku, Osaka 545-8585, Japan*

Correspondence should be addressed to Eiji Ishimura, ish@med.osaka-cu.ac.jp

Received 21 June 2011; Revised 2 August 2011; Accepted 4 August 2011

Academic Editor: Yasuhiko Tomino

To evaluate proteins associated with the development of diabetic nephropathy, a major cause of the end-stage renal disease, we analyzed protein expression in isolated glomeruli from spontaneous type 2 diabetic (OLETF) rats and their age-matched control littermates (LETO) in the early and proteinuric stages of diabetic nephropathy using QSTAR Elite LC-MS/MS. Among the 191 and 218 proteins that were altered significantly in the OLETF rats, twenty-four were actin cytoskeleton-associated proteins implicated in the formation of stress fibers, and the impairment of actin polymerization, intermediate filaments and microtubules. Importantly, sorbin and SH3 domain containing 2 (SORBS2), which is involved in the formation of stress fibers, was significantly upregulated in both stages of diabetic nephropathy (1.49- and 1.97-fold, resp.). Immunohistochemical and quantitative-PCR analyses revealed upregulation of SORBS2 in podocytes of glomeruli of OLETF rats. Our findings suggested that SORBS2 may be associated with the development of diabetic nephropathy possibility by reorganization of actin filaments.

1. Introduction

Diabetes mellitus accounts for more cases of end-stage renal disease than any other cause of chronic kidney disease [1]. While glomerular hypertrophy, mesangial matrix expansion, and glomerular basement membrane (GBM) thickening are the classical hallmarks of diabetic glomerular lesions, studies of diabetic patients and animal models have revealed that the onset of proteinuria is most closely associated with podocytopathies, such as podocyte apoptosis, hypertrophy, detachment from the GBM, and foot process effacement [2]. Indeed, diabetic nephropathy is now recognized as one of the major podocyte-associated diseases [3]. The podocyte is an excellent model system for studying actin cytoskeleton dynamics in a physiological context because changes in actin dynamics transfer directly into changes of kidney function [4]. Previous investigations have shown that the cytoskeleton on the GBM side in podocytes during foot process effacement is comprised of highly-ordered, actin-based bundles that run parallel to the longitudinal axis of the foot processes [4] and that actin fibers gather to form the stress fibers [4, 5]. Therefore, reorganization of the actin filaments is indispensable for foot process effacement.

Sorbin and SH3 domain containing 2 (SORBS2), alpha-actinin 1 (ACTN1), alpha-actinin 4 (ACTN4) and Rho GDP dissociation inhibitor alpha (ARHDGDIA) are proteins associated with stress fiber formation [6–11]. The relationship between these proteins and diabetic nephropathy has not been elucidated, although some of these proteins have been reported to be important in stress fiber formation in podocytopathies or proteinuria [4, 8, 9, 12]. The underlying cytoskeletal components that initiate and regulate the dynamic changes of these foot processes remain unclear.

Recently, proteome analysis has increasingly been used in the discovery of disease-specific proteins and biomarkers of kidney diseases [13, 14]. Proteome analysis of diabetic glomeruli from renal biopsy specimens of diabetic patients is difficult, due to the fact that renal biopsy is clinically limited in diabetic patients, and only small (often insufficient) quantities of glomeruli can be obtained from renal biopsy specimens. From these concerns, in order to reveal which proteins are involved in the diabetic glomerular alterations, including podocytopathies, we conducted a proteome analysis of isolated glomeruli from spontaneous type 2 diabetic (Otsuka Long-Evans Tokushima Fatty (OLETF)) rats and their age-matched control littermates (Long-Evans Tokushima Lean (LETO)) rats at 27 (early stage of diabetic nephropathy) and 38 (proteinuric stage of diabetic nephropathy) weeks of age using QSTAR Elite liquid chromatography with tandem mass spectrometry (QSTAR Elite LC-MS/MS) and iTRAQ technology.

2. Materials and Methods

2.1. Animals. All experimental procedures were conducted after obtaining approval of the Animal Care and Use Committee of the Osaka City University Medical School and in accordance with the Guide for Laboratory Animals. OLETF and LETO rats (n = 20, resp.) were provided by Otsuka Pharmacology Co., Ltd. (Tokushima, Japan). The diabetic phenotype of the OLETF rat has been extensively evaluated: (i) 25-week-old rats develop diabetes (hyperglycemia, hyperlipidemia, etc.) at nearly 100% incidence and (ii) 30-week-old rats develop proteinuria [15]. Therefore, we assumed that OLETF rats develop diabetic nephropathy with the early and the proteinuric stages at 27 and 38 weeks of age, respectively. 10 OLETF rats and 10 LETO rats were used for analysis at each time point. All animals were housed individually in each cage in an animal facility maintained on a 12-h (7:00–19:00) light/dark cycle, at a constant temperature of 23 ± 1°C and relative humidity of 44 ± 5% for 21 and 32 weeks, respectively, from the start of the experiment and were provided tap water and food (rodent pellet diet MF 348 kcal/100 g, containing 4.2% crude fat; Oriental Yeast Co., Tokyo, Japan) ad libitum.

2.2. Biochemical Characterization. Total cholesterol and creatinine in serum specimens (n = 10/group), hemoglobin A1c, fasting plasma glucose concentrations in plasma specimens (n = 10/group), and protein and creatinine concentrations in spot urine samples (n = 5/group) were measured using an autoanalyser (Mitsubishi Chemical Medience Co., Ltd., Osaka, Japan).

2.3. Histopathological Examination. Renal tissues were fixed in 10% neutral formalin solution, embedded in paraffin, and cut into 3 μm sections using conventional techniques. Sections were stained with hematoxylin and eosin and periodic acid-Schiff (PAS) reagent and examined histopathologically by light microscopy.

2.4. Glomerular Isolation. Rats were anesthetized with intraperitoneal injection of pentobarbital (60 mg/kg) for euthanasia and necropsy. After laparotomy, the kidneys were perfused with ice-cold phosphate-buffered saline (PBS) until they were blanched. Glomeruli were isolated by a sieving technique, as described previously [16, 17]. Isolated glomeruli were collected under an inverted microscope to minimize tubular contamination (less than 5% tubular fragments) and centrifuged at 453 g for 10 min. The pellets were collected and used for proteome analysis.

2.5. Lysis and Digestion, iTRAQ Labeling, and LC-ESI MS/MS Analysis. The lyophilized samples were dissolved in 1000 μL tissue protein extraction reagent lysis buffer (Pierce, IL, USA) with protease inhibitor (p8340, Sigma-Aldrich). The glomerular lysates were ultrasonicated and insoluble material was removed by centrifugation at 13,000 g for 15 min at 10°C. Protein concentrations were quantified using the BCA Protein Assay kit (Pierce, Ill, USA). Protein reduction, alkylation, digestion and subsequent peptide labeling were performed using the AB Sciex iTRAQ Reagent Multi-Plex Kit (AB Sciex, Foster City, Calif, USA) according to the manufacturer's instructions with minor modifications [18, 19]. Briefly, 50 μg samples of protein were incubated at 60°C for 60 min in 20 μL dissolution buffer (0.5 M triethylammonium bicarbonate, 0.2% SDS) with 2 μL reducing reagent (50 mM tris(2-carboxy-ethyl)phosphine). Free cysteine sulfhydryl groups were blocked by incubation with 1 μL cysteine blocking reagent (20 mM methyl methanthiosulfonate) at room temperature for 10 min. Ten μL of trypsin solution (AB Sciex, Foster City, Calif, USA) was added, and each sample was incubated overnight at 37°C. Samples from OLETF and LETO rats were labeled with iTRAQ114 and iTRAQ115, respectively, and then mixed into one tube and fractionated using six concentrations of KCl solutions (10, 50, 70, 100, 200, and 350 mM) on an ICAT cation exchange cartridge (AB Sciex, Foster City, Calif, USA). After desalting and concentrating, peptides in each fraction were quantified by a DiNa-AI nano LC System (KYA Technologies, Tokyo, Japan) coupled to a QSTAR Elite Hybrid MS/MS spectrometer through a Nanospray ion source (AB Sciex, Foster City, Calif, USA), as described previously [19].

2.6. Identification of Proteins by IPA. Protein Pilot 2.0 software with the Paragon Algorithm (AB Sciex, Foster City, Calif, USA) was used for the identification and relative quantification of proteins. Tandem mass spectrometry data were compared against the rat protein database from Swiss-Prot 57.4 (20,400 sequences). We report only protein identifications with >95% statistical confidence in the Protein Pilot 2.0 software.

The Ingenuity Analysis (IPA; Ingenuity Systems, Mountain View, Calif, USA) was utilized to identify networks of interacting proteins, functional groups, and pathways. Information regarding the function and cellular localization of the identified proteins was obtained from IPA.

2.7. Immunohistochemistry for SORBS2. Immunohistochemical staining of the kidney sections was performed according to the avidin-biotin complex method, as described

previously [20], using primary mouse monoclonal anti-rat SORBS2 (clone S5C, Sigma-Aldrich), After deparaffinization with xylene and gradual dehydration, antigen retrieval was undertaken by microwaving in sodium citrate buffer (pH 6) for 25 min and endogenous peroxidase activity was blocked by 3% hydrogen peroxide for 5 min. Sections were incubated with 1.5% normal horse or goat serum in PBS for 15 min and then with diluted primary antibody (1 : 500), overnight at 4°C. Biotinylated horse anti-mouse antibodies (diluted 1 : 200) were applied as the secondary antibodies for 30 min, and the slides were then incubated with the avidin-biotin peroxidase complex for 30 min. The peroxidase reaction was developed using 0.02~0.033% 3,3-diaminobenzidine tetrahydrochloride (DAB) and 0.03% hydrogen peroxide in tris-buffered saline for 1–5 min. Hematoxylin was used for counterstaining.

2.8. Immunofluorescence for SORBS2 and Synaptopodin. Double immunofluorescence of SPRBS2 and synaptopodin, a podocyte marker proteins was performed as previously described [21–23]. Four-μm-thick frozen kidney tissue sections were fixed with ice-cold acetone at −20°C for 5 min, followed by permeabilization with 1% Tween 20 PBS for 5 min at room temperature. After rinsing with 1% Tween 20 PBS, unspecific binding sites were blocked with horse anti-mouse and goat anti-rabbit serum in PBS for at least 30 min. Primary antibodies (prediluted in blocking solution) for SORBS2 (1 : 250) and synaptopodin (clone ab 101883, Abcam) (1 : 300) were applied for 60 min at room temperature, followed by incubation with the secondary antibody fluorescein red-conjugated horse anti-mouse IgG (Alexa Fluor 594) (Life technologies, Calif, USA) and fluorescein green-conjugated goat anti-rabbit IgG (Alexa Fluor 488) (Life technologies, Calif, USA) for 30 minutes at room temperature. Spatial colocalization of SORBS2 immunoreactivity (red fluorescence) with synaptopodin (green fluorescence), resulting in yellow, was obtained by overlaying separately recorded images on a color image. The immunofluorescence was analyzed by confocal microscopy with the help of the Fluoview software (Olympus Optical, Tokyo, Japan).

2.9. Validation of SORBS2 mRNA Expression by Real-Time Quantitative PCR (Q-PCR)

2.9.1. RNA Preparation. Glomeruli from OLETF and LETO rats at the proteinuric stage (n = 3, resp.) were laser-microdissected using the ZEISS PALM MB4 Microdissection System (ZEISS, Munich, Germany), according to the manufacturer's instructions. Total RNA was isolated from glomeruli using 4 M guanidine thiocyanate, 25 mM sodium citrate with 0.5% sarkosyl buffer with the phenol-chloroform-isoamyl alcohol extraction method, using glycogen as a carrier, as described previously [24]. Reverse transcription of total RNA was performed with Oligo-dT primer, and cDNA samples were stored at −20°C until assayed.

2.9.2. Real-Time Q-PCR. PCR amplicons were used to confirm SORBS2 gene expression using real-time Q-PCR. Primer sequences were designed with the Primer Express software (Applied Biosystems, USA). The probes and primers were as follows: TaqMan probe and primer set Rn00587190_m1 for SORBS2 (NM_053770.1) and TaqMan probe 5′-TGA GAC CTT CAA CAC CCC AGC CAT G-3′, and primers: forward 5′-TCA AAT AAG CCA CAG CGT C-3′, reverse 5′-AAC CAG CCG TCAT CACA C-3′ for GAPDH, cytoplasmic (NM_ 017008.3). The cDNA generated from each sample was used for Q-PCR according to the manufacturer's instructions, with GAPDH as an internal control.

2.10. Ultrastructural Examination. Separate portions of the kidneys from the OLETF and LETO rats (n = 5, resp.) at 38 weeks of age were also prepared for electron microscopy. Specimens were obtained from the renal cortex, fixed in 0.1 M cacodylate buffer solution (pH 7.4) containing 3% glutaraldehyde, and postfixed in the same buffer containing 1% osmium tetroxide at 4°C, as previously described [25]. Seventy nm sections were stained with uranyl acetate and lead citrate for examination using a JEM 1200 EXII electron microscope (JEOL, Tokyo, Japan).

2.11. Statistical Analysis. Statistical calculations were performed using Graph-Pad Prism version 5.0 for Windows (Graphpad Software, San Diego, Calif). For normally distributed data, statistical significance ($P < 0.05$) was evaluated using the unpaired t-test followed by an analysis of variance (F-test). In the case of statistically significant differences regarding variances, the Welch test was used to confirm the differences between groups. For nonparametric testing, the Mann-Whitney U-test was applied. The results are presented as box plots/dot plots. All values are expressed as the means ± SD. For analysis of protein expression, statistical analysis with Protein Pilot 2.0 software was employed.

3. Results

3.1. General Observations. The OLETF rats exhibited polyphagia and obesity from the very early stages of life. At 27 weeks of age (early stage of diabetic nephropathy), the mean body weight of the OLETF rats (642±40.9 g) was significantly higher than that of the LETO rats (491 ± 34.6 g). At 38 weeks of age (proteinuric stage of diabetic nephropathy), the body weights of the LETO rats were increased, although the final values for the OLETF (621 ± 69.4 g) and the LETO (580 ± 80.7 g) rats were not significantly different. At both time points, the kidney-to-body weight ratio of the OLETF rats (27 weeks: 0.703% ± 0.10%, 38 weeks: 0.780% ± 0.12%) was significantly higher than that of the LETO rats (0.597% ± 0.054% and 0.592% ± 0.050%, resp.).

The mean blood glucose, hemoglobin A1c and total cholesterol levels in the OLETF rats (27 weeks: 183 ± 58.9 mg/dL, 4.4 ± 0.85%, 123 ± 23.1 mg/dL, 38 weeks: 248 ± 53.6 mg/dL, 5.7% ± 1.2%, and 153 ± 34.6 mg/dL, resp.) were increased significantly compared with those in the LETO rats (27 weeks: 135 ± 34.2 mg/dL, 3.3% ± 0.11%, 97.4 ± 9.5 mg/dL, 38 weeks: 129 ± 25.3 mg/dL, 3.3% ± 0.18%, and 101 ± 9.37 mg/dL, resp.). The serum creatinine levels were

Table 1: Biological parameters from OLETF and LETO rats at 27 and 38 weeks of age.

	OLETF ($n = 10$)	LETO ($n = 10$)	P value	OLETF ($n = 10$)	LETO ($n = 10$)	P value
	27 weeks			38 weeks		
Body weight (g)	642 ± 40.9	491 ± 34.6	<0.0001	621 ± 69.4	580 ± 80.7	0.2089
Food intake (g/day)	34.9 ± 6.1	19.1 ± 1.5	<0.0001	39.3 ± 6.1	29.7 ± 2.0	<0.0001
Kidney-to-body weight ratio (%)	0.703 ± 0.10	0.597 ± 0.054	0.0091	0.780 ± 0.12	0.592 ± 0.050	0.0008
Fasting plasma glucose (mg/dL)	183 ± 58.9	135 ± 34.2	00388	248 ± 53.6	129 ± 25.3	<0.0001
Hemoglobin A1c (%)	4.4 ± 0.85	3.3 ± 0.11	0.0021	5.7 ± 1.2	3.3 ± 0.18	0.0001
Total cholesterol (mg/dL)	123 ± 23.1	97.4 ± 9.5	0.0081	153 ± 34.6	101 ± 9.37	0.0009
Creatinine (mg/dL)	0.24 ± 0.04	0.36 ± 0.04	<0.0001	0.33 ± 0.05	0.46 ± 0.1	0.0031
Urinary protein-to-creatinine ratio (mg/mg)	2.73 ± 2.10 ($n = 5$)*	0.60 ± 0.08 ($n = 5$)*	<0.0001	5.65 ± 2.36 ($n = 5$)*	0.94 ± 0.38 ($n = 5$)*	<0.0001

Values are expressed as the mean ± SD.
*Urinary specimens were obtained from 5 rats per group to measure urinary protein and creatinine levels.
OLETF: Otsuka Long-Evans Tokushima Fatty, LETO: Long-Evans Tokushima Lean.

significantly higher at both nephropathy stages for LETO rats (27 weeks: 0.36 ± 0.04 mg/dL and 38 weeks: 0.46 ± 0.10 mg/dL) compared with the OLETE rats (0.24 ± 0.04 mg/dL and 0.33 ± 0.05 mg/dL). The urinary protein to creatinine ratio in the OLETF rats was also elevated significantly at both time points examined (27 weeks: 2.73 ± 2.10 mg/mg and 38 weeks: 5.65 ± 2.36 mg/mg) compared with the LETO rats (0.60 ± 0.08 mg/mg and 0.94 ± 0.38 mg/mg) (Table 1).

3.2. Histopathological Examination. In the OLETF rats, histopathological examination demonstrated both focal and segmental glomerular changes. Slight expansion of the mesangial matrix was observed with mesangial cell proliferation at 27 weeks of age (Figure 1(a)). At 38 weeks of age, in addition to the mesangial area, a few glomeruli exhibited segmental lesions with PAS-positive deposits in the mesangium or capillary that resembled the fibrin caps commonly observed in exudative lesions in human diabetic nephropathy (Figure 1(c)). In the LETO rats, there were no obvious histopathological changes at both time points (Figures 1(b) and 1(d)).

3.3. Alterations of Protein Expression in Glomeruli from Diabetic Rats. The results of QSTAR Elite LC-MS/MS and Protein Pilot analyses are summarized in Table 2. Altered expression of 191 (91 up- and 100 downregulated) and 218 (121 up- and 97 downregulated) proteins was observed in isolated glomeruli from OLETF rats at the early and proteinuric stages of diabetic nephropathy, respectively. These proteins were involved in glycolysis, oxidative stress, and podocyte injury, based upon the IPA findings (Figure 2).

Eighty-seven proteins were differentially expressed in isolated glomeruli from OLETF rats compared with those from LETO rats at both stages of diabetic nephropathy. Among these 87 proteins, 24 were involved in actin cytoskeleton reorganization, that is, formation of stress fibers (SORBS2, ACTN1, ACTN4 and ARHGDIA), polymerization of actin filaments (actin-related protein 2/3 complex subunit 1 beta (ARPC1B), actin-related protein 2/3 complex subunit 5 (ARPC5), actin-related protein 3 homolog (ACTR3), myristoylated alanine rich kinase C substrate (MARCKS), and adducin 1 alpha (ADD1)), microtubules (tubulin alpha 1c (TUBA1C) and dynein cytoplasmic 1 (DYNC1)) intermediate filaments (vimentin (VIM), lamin A/C (LMNA), desmin (DES), nestin (NES) and plectin1 (PLEC1)), formation of GBM (integrin beta 1 (INTGB1), vinculin (VCL) and agrin (AGRN)), and other actin-binding proteins (plastin 3 (PLS3), spectrin alpha non-erythrocytic 1 (SPTAN1), calponin 3 (CNN3), tropomyosin 3 (TPM3) and ezrin (EZR)). Among these proteins, Table 2 presents the actin cytoskeleton-associated proteins with high- or low-fold changes of more than 20% (average iTRAQ ratio >1.20 or <0.83) and P values less than 0.05. SORBS2 was the only upregulated protein in glomeruli from OLETF rats at both the early and the proteinuric stages of diabetic nephropathy.

3.4. Confirmation of SORBS2 Expression by Immunohistochemistry. Figures 1(e), 1(f), 1(g), and 1(h) show representative immunostaining results for the SORBS2. There were no clear differences in the expression of SORBS2 between the OLETF and LETO rats at 27 weeks of age (Figures 1(e) and 1(f)). However, SORBS2 was clearly observed in podocytes from OLETF rats at 38 weeks of age (Figures 1(g) and 1(h)).

Immunofluorescence of SPRBS2 and synaptopodin are shown in Figure 3. SORBS2 was observed in glomeruli from OLETF rats at 38 weeks of age (Figure 3(a)). Synaptopodin was observed in glomeruli from OLETF rats at 38 weeks of age (Figure 3(b)). When the stainings of SORBS2 and synaptopodin were merged, they showed as a capillary pattern in glomeruli from OLETF rats at 38 weeks of age (Figure 3(c)).

3.5. SORBS2 mRNA Expression in Isolated Glomeruli. To determine whether SORBS2 localizes within glomeruli and to assess changes of its expression, real-time Q-PCR analyses were also performed. Consistent with the QSTAR proteome analysis results, a tendency towards increased SORBS2

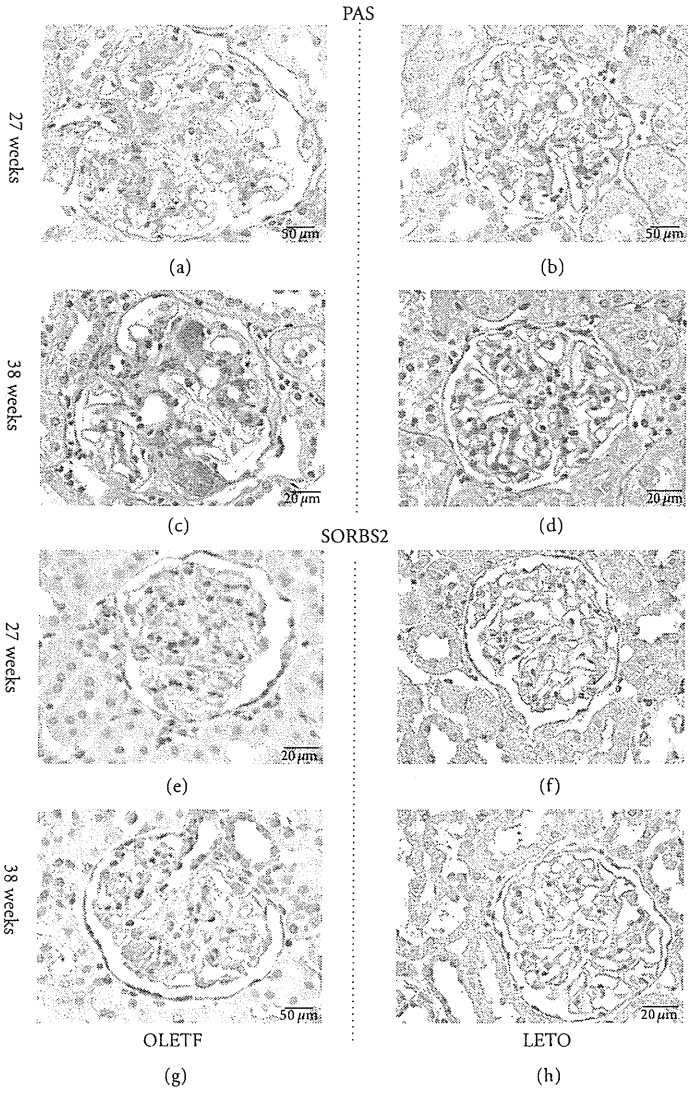

FIGURE 1: Periodic acid Schiff (PAS) and immunohistochemical staining in the kidneys from OLETF (a, c, e, and g) and LETO (b, d, f, and h) rats at 27 and 38 weeks of age. Slight expansion of the mesangial matrix with mesangial cell proliferation (a). Normal glomeruli (b). Exudative and sclerotic lesion (c). Normal glomeruli (d). SORBS2 positivity in podocytes from OLETF rats (e, f) and negativity in those from LETO rats (f, h). Scale bar = 20 μm.

mRNA expression in glomeruli from OLETF rats was observed compared to those from LETO rats (1.76 ± 0.15 versus 1.40 ± 0.19, $P = 0.06$).

3.6. Ultrastructural Examination Using Electron Microscopy. To validate the podocyte foot process effacement in the OLETF rats, ultrastructural examination was performed at 38 weeks of age. At this time, foot process effacement was not observed in the LETO rats, but was obvious in the OLETF rats (Figures 4(a) and 4(b)). These results and the urinary protein-to-creatinine ratio (5.65 ± 2.36 mg/mg) indicated that 38 weeks of age is appropriate for the detection of the proteinuric stage of diabetic nephropathy in the OLETF rats.

4. Discussion

In the present study, we performed a targeted proteome analysis of glomeruli isolated from rats in both the early (27 weeks of age) and the proteinuric (38 weeks of age) stages of diabetic nephropathy. It is reported that proteins quantified with a fold change of more than 20% (average iTRAQ ratio >1.20 or <0.83) and a P value less than 0.05 were identified as differentially expressed proteins [26, 27]. We demonstrated changes of many kinds of proteins in isolated glomeruli from diabetic rats; these proteins participate in glycolysis, citric acid cycle, formation of oxidative stress, and other intracellular processes, as shown in Figure 2. The results of IPA demonstrated that 17 actin cytoskeleton-associated

Table 2: Differentially expressed actin cytoskeleton-associated proteins in glomeruli isolated from OLETF and LETO rats, identified by QSTAR Elite LC-MS/MS and IPA.

Protein	GI number	Mass (Da)	Location	Function	Foldchange (27 weeks)	*P* value	Fold change (38 weeks)	*P* value
Stress fiber formation								
Sorbin and SH3 domain containing 2 (SORBS2)	205831248	124108	C	AD	1.49	<0.0001	1.97	<0.0001
Alpha-actinin 1 (ACTN1)	13123942	103058	C	ST, CL	1.02	0.764	1.40	<0.0001
Alpha-actinin 4 (ACTN4)	182705246	104654	C	ST, CL	0.93	0.46	1.22	<0.0001
Rho GDP dissociation-inhibitor alpha (ARHGDIA)	21759130	23207	C	RI	1.28	0.041	0.87	0.0413
Actin-filament polymerization								
Actin-related protein 2/3 complex subunit 1 beta (ARPC1B)	12229626	40950	C	AP, EC	0.65	0.0363	0.73	0.0136
Actin related protein 2/3 complex subunit 5 (ARPC5)	3121767	16320	C	AP, EC	0.72	0.0014	0.74	0.0002
Myristoylated alanine-rich protein kinase C substrate (MARCKS)	266495	31555	UN	AP	0.60	0.0004	0.71	0.002
Microtubules formation								
Tubulin alpha 1c (TUBA1C)	55976169	49895	C	MT	0.74	0.012	0.90	0.17
Intermediate filaments formation								
Lamin A/C (LMNA)	1346413	74139	N	IF	0.89	0.0076	1.29	<0.0001
Desmin (DES)	1352241	53536	C	IF	0.94	0.143	1.32	<0.0001
Nestin (NES)	146345465	177439	C	IF	0.83	<0.0001	1.03	0.32
Plectin 1 (PLEC1)	1709655	531791	C	IL	0.82	<0.0001	0.96	0.12
GBM (glomerular basement membrane)								
Integrin beta 1 (INTGB1)	1352494	15105	PM	APG	0.82	0.0015	0.92	0.0094
Agrin (AGRN)	399021	214846	PM	LB	0.62	0.042	0.90	0.490
Others								
Plastin 3 (PLS3)	226693553	70811	C	CL	0.82	0.02	0.82	0.0005
Calponin 3 (CNN3)	584956	36414	C	AB	0.60	0.0013	0.78	0.088
Tropomyosin 3 (TPM3)	148840439	32819	C	AS	0.71	<0.0001	0.80	<0.0001

AB: actin binding; AD: adaptor protein; AP: actin filament polymerization; APG: anchoring podocyte and GBM (glomerular basement membrane); AS: actin filaments stabilization; C: cytoplasm; CL: crosslinking actin filaments into bundles or networks; EC: endocytosis; IF: intermediate filaments; IL: interlinks; LB: laminin binding; LETO: Long-Evans Tokushima Lean; MT: microtubules; N: nuclear; OLETF: Otsuka Long-Evans Tokushima Fatty; PM: plasma membrane; RI: Rho GDP-dissociation-inhibitor activity; ST: stress fibers; UN: unknown.

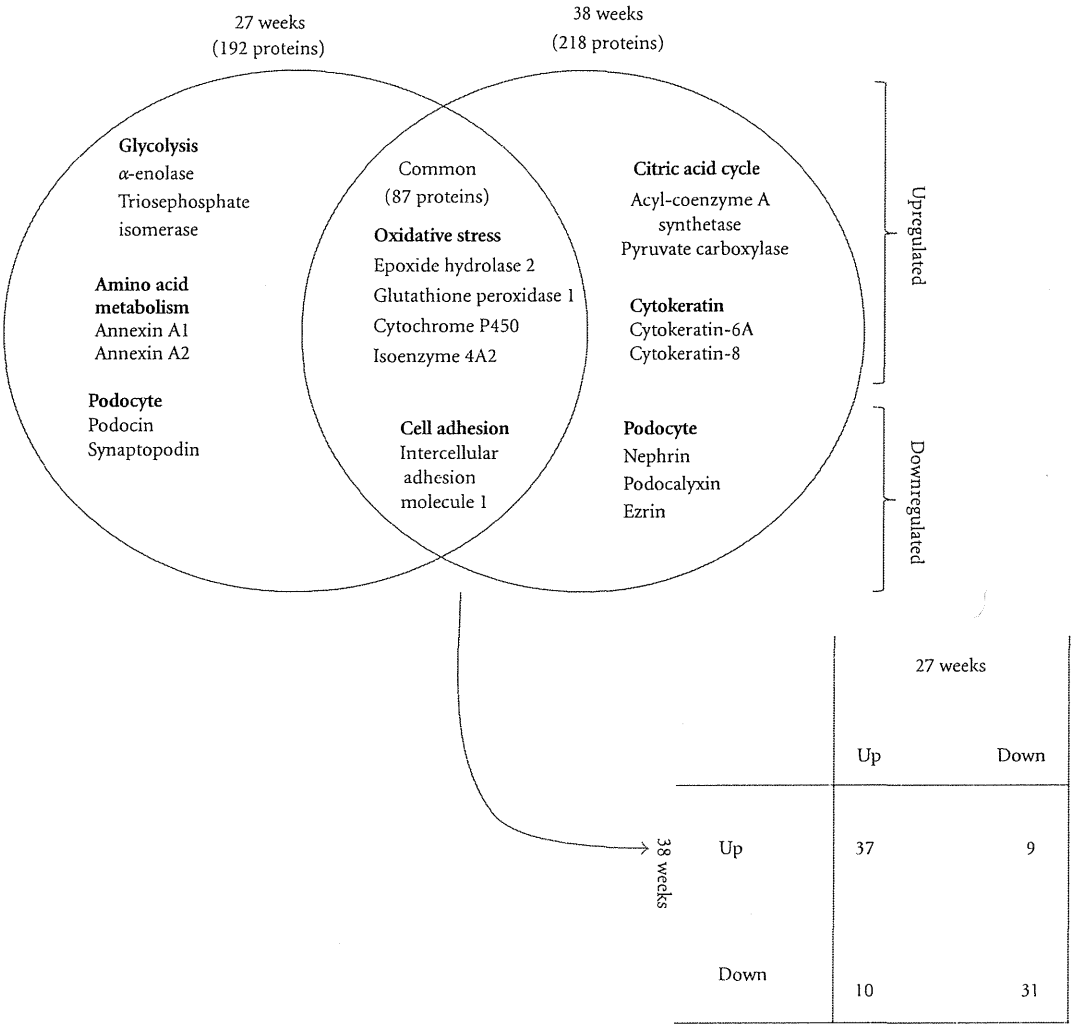

FIGURE 2: Comparative analysis of subclasses of differentially expressed proteins, excluding actin cytoskeleton-associated proteins, in the kidneys from OLETF and LETO rats at 27 and 38 weeks of age, by the Ingenuity Pathway Analysis (IPA).

proteins were significantly and differentially expressed between OLETF and LETO rats.

Among these proteins that were differentially expressed in isolated glomeruli from OLETF and LETO rats at both 27 and 38 weeks of age were SORBS2 (upregulated), ARCP1B (downregulated), ARPC5 (downregulated), MARCKS (downregulated), PLAS3 (downregulated), CNN3 (downregulated), and TPM3 (downregulated). SORBS2 was the only up-regulated protein in glomeruli from OLETF rats at both the early and the proteinuric stages of diabetic nephropathy, compared to those from LETO rats. There have been no previous reports suggesting any relationship between SROBS2 and diabetic nephropathy.

SORBS2 is an Arg/Abl-binding protein that contains three COOH-terminal Src homology 3 domains, a serine/threonine-rich domain, and several potential Abl phosphorylation sites. It is widely expressed in human tissues, such as heart, brain, spleen, pancreas, and kidney. In epithelial cells, SORBS2 is located in stress fibers [28]. In addition, SORBS2 has been reported to function as an adapter protein in the assembly of signaling complexes in stress fibers and as a potential link between the Abl family kinases and the actin cytoskeleton [8, 9]. In the present study, SORBS2 was up-regulated in isolated glomeruli from OLETF rats based upon proteome analysis using the QSTAR Elite LC-MS/MS. Although there was a tendency towards increased levels of SORBS2 mRNA in microdissected glomeruli from OLETF rats, we confirmed its localization in diabetic glomeruli, especially in podocytes of OLETF rats at the proteinuric stage using immunohistochemistry. Considering the previously reported functions of SORBS2 and the alterations of SORBS2 expression observed in the present study, SORBS2 may be associated with the development of diabetic nephropathy by reorganization of actin filaments, including actin stress fiber formation.

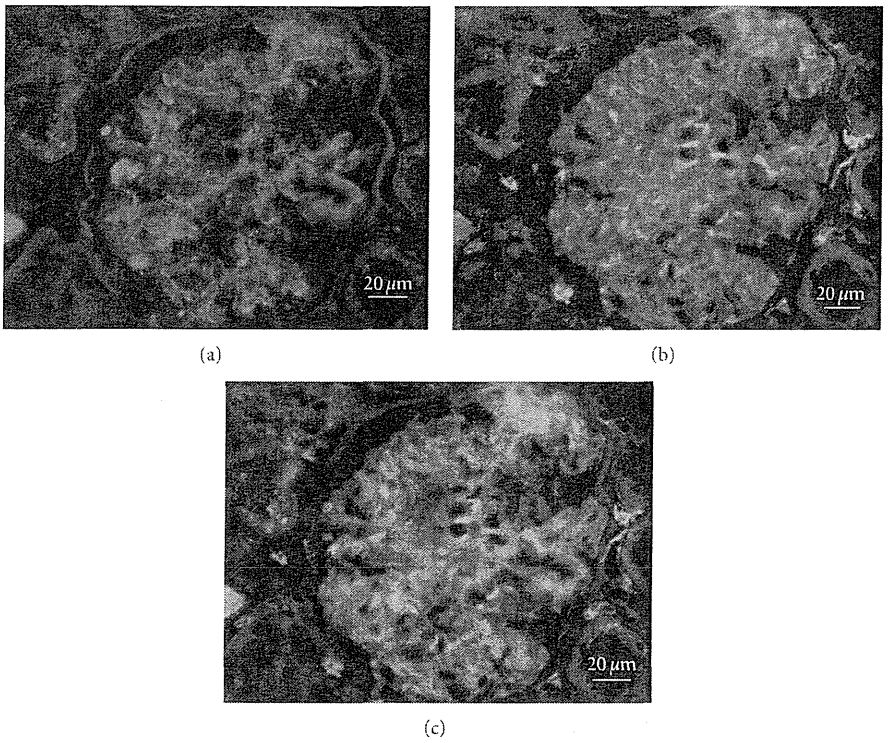

(a) (b)

(c)

FIGURE 3: Immunofluorescence for SORBS2: red (a), synaptopodin: green (b), and merge SORBS2 and synaptopodin: yellow (c) in OLETF rats at 38 weeks of age. SORBS2 was expressed as a capillary pattern in glomeruli from OLETF rats at 38 weeks of age. Scale bar = 20 μm.

ARCP1B, ARPC5, and MARCKS are actin filament polymerization-related proteins. During polymerization of actin filaments, binding of the Arp2/3 complex to the sides of actin filaments is important for its actin nucleation and branching activities [29]. MARCKS substrate is located at glomeruli, specifically to podocytes, and controls both actin polymerization and actin cytoskeleton binding to the membrane [30]. Alterations of crosslinking proteins that organize actin filaments into bundles or networks, that is, PLS3 (I-plastin), were also detected in the present study. PLS3 is an actin-binding protein expressed in the kidney, that is, known to be located in stress fibers [31] and has been reported to be related to minimal change nephritic syndrome [32]. Moreover, CNN3 plays a direct role in cell contractility in vivo and controls the cytoskeletal composition of podocytes [33]. TPM3 binds to actin filaments and has been implicated in their stabilization [34]. These protein changes may be related to the collapse of actin filaments and the disentanglement of actin bundles or networks of diabetic glomeruli in the early and proteinuric stages of diabetic nephropathy.

ACTN4 is widely expressed in podocyte foot processes and is colocalized with actin stress fibers [6]. The Upregulation of ACTN4 observed during the proteinuric stage in the present study is consistent with a previous report [10]. ACTN1 is present in multiple subcellular regions, including cell-cell and cell-matrix contact sites, cellular protrusions, lamellipodia, and stress fiber dense regions [35], and cross-links actin filaments within stress fibers [11]. ACTN1 was also up-regulated in glomeruli from OLETF rats at 38 weeks of age. ARHGDIA maintains the Rho family members (Rac1, Cdc42, and RhoA), which promote the assembly of actin-myosin filaments and cell stress fibers in the GDP-bound inactive form. Mice lacking ARHGDIA are initially viable and healthy but develop massive proteinuria and glomerulosclerosis later in life [7, 10]. Upregulation of ARHGDIA in the early stage might indicate suppression of the Rho family members. Coincident with the Upregulation of SORBS2 at both stages of OLETF rats in the present study, changes in these protein expression patterns may be associated with reorganization of actin filaments, leading to foot process effacement and the progression of diabetic nephropathy. In the present study; however, we could not validate the expression of ACTN4 and ARGDIA in OLETF rats.

In addition to increasing stress fibers, the impairment of polymerization of actin filaments, intermediate filaments and microtubules, disentanglement of actin filaments, and podocyte detachment from the GBM are also key events for podocytopathies. Intermediate filaments and microtubules are known to form the scaffold of major podocyte processes and the central cell body [36]. NES and PLEC1 were down-regulated in the kidneys from OLETF rats at 27 weeks of age, indicating the collapse or the disentanglement of intermediate filaments and microtubules in the early stage of diabetic nephropathy. Furthermore, podocytes are attached

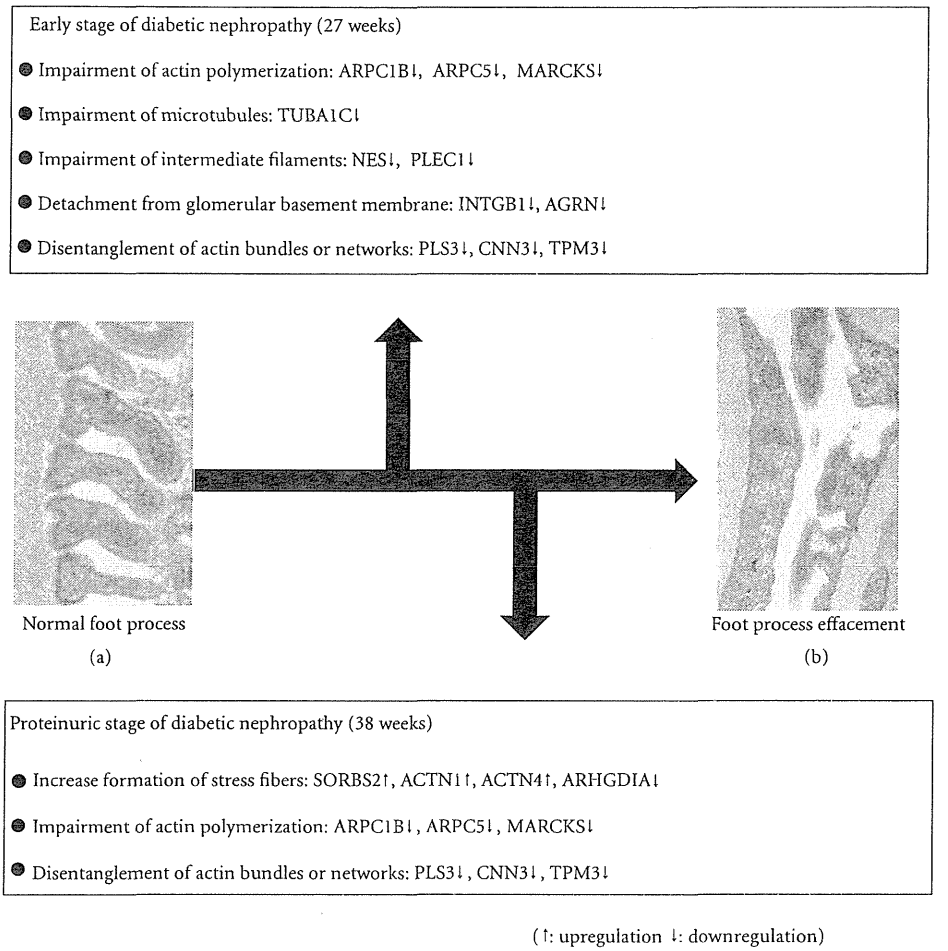

FIGURE 4: Alterations in protein expression during podocyte foot process effacement in diabetic nephropathy. Electron micrograph of podocytes from OLETF and LETO rats at 38 weeks of age. LETO rats (×40,000) (a), OLETF rats (×40,000) (b).

to the outer aspect of the GBM and their foot processes are connected to the GBM [37]. Downregulation of INTGB1 and AGR may indicate that podocytes are detached from the GBM, resulting in foot process effacement and proteinuria.

The alterations of proteins observed in this study are summarized in Figure 4. Based on proteome analysis of isolated glomeruli from diabetic rats, the following changes of the cytoskeleton at the early and proteinuric stages of diabetic nephropathy could occur: (1) increased formation of stress fibers during the proteinuric stage of diabetic nephropathy, (2) impairment of actin polymerization at both time points, suggesting collapse or dysfunction of actin filaments, (3) decreased expression of proteins associated with microtubules and intermediate filaments during both the early and the proteinuric stages, (4) decreased GBM cytoskeleton-associated proteins at both stages, suggesting podocytopathies, and (5) collapse or disentanglement of actin filaments at both stages. Our findings suggested that impairment or collapse of actin filaments may cause podocyte foot process effacement (Figure 4(b)) and the emergence of proteinuria in diabetic nephropathy. As observed in the present study, increases in stress fibers at the proteinuric stage may be related to reorganization of actin filaments [4, 5]. Proteome analysis demonstrated that numerous cytoskeleton-associated proteins could contribute to the onset and/or progression of diabetic nephropathy.

There are some limitations in the present study. First, in the glomerular isolation, we used a sieving method to minimize tubular contamination. Despite the implementation of this technique and effort, it is impossible to completely avoid tubular contamination. Indeed, one of the mitochondrial proteins, that is, mitochondrial import inner membrane translocase subunit 44 (TIM44), which is activated in diabetic nephropathy [38] was up-regulated in OLETF rats at 27 weeks of age (fold change 1.34, $P = 0.04$). A second limitation is the protein detection using the QSTAR Elite LC-MS/MS. Although, some podocyte-related proteins, such as podocin and synaptopodin, were downregulated in OLETF rats at 27 weeks of age (fold change 0.83 $P = 0.001$; fold change 0.63, $P = 0.0001$, resp.), these proteins were not detected in OLETF rats at 38 weeks of age, due to mechanical problems or problems with

reproducibility of protein identification using the QSTAR Elite LC-MS/MS. Lastly, although proteome analysis is one of the most powerful and useful tools in the detection of novel proteins for various kidney diseases, it requires validation or further mechanical analysis of the results of proteome analysis. Although there are some limitations in the present methodology, our findings demonstrated the usefulness of proteome analysis of isolated glomeruli, which allows the direct and comprehensive investigation of protein alterations of diabetic glomeruli.

In conclusion, the present proteome analysis demonstrated that numerous cytoskeleton-associated proteins contribute to the onset and/or progression of diabetic nephropathy. This proteome study also demonstrated, for the first time, that SORBS2 expression was increased in diabetic glomeruli and suggested that SORBS2 may be associated with the development of diabetic nephropathy by reorganization of actin filaments, along with other actin cytoskeleton-associated proteins. Further investigation is necessary to ascertain the significance of SORBS2 and these actin cytoskeleton-associated proteins in diabetic nephropathy.

Conflict of Interests

The authors declared that they have no conflict of interests.

Abbreviations

ACTN1:	Alpha-actinin 1
ACTN4:	Alpha-actinin 4
AGRN:	Agrin
ARHGDIA:	Rho GDP dissociation-inhibitor alpha
ARPC1B:	Actin-related protein 2/3 complex subunit 1 beta
ARPC5:	Actin-related protein 2/3 complex subunit 5
CNN3:	Calponin 3
DES:	Desmin
GBM:	Glomerular basement membrane
INTGB1:	Integrin beta 1
LMNA:	Lamin A/C
MARCKS:	Myristoylated alanine rich protein kinase C substrate
NES:	Nestin
PLEC 1:	Plectin 1
PLS3:	Plastin 3
SORBS2:	Sorbin and SH3 domain containing 2
TPM3:	Toropomyosin 3
TUBA1C:	Tubulin alpha 1c.

Acknowledgments

The authors thank Dr. Naomi Ishii, Ms. Azusa Inagaki, Ms. Kaori Touma, and Ms. Rie Onodera for their technical assistance and Ms. Yukiko Iura for her help during the preparation of this paper. This work was supported by a Grant-in-Aid for Scientific Research of The Ministry of Education, Culture, Sports, Science and Technology (no. 23591198).

References

[1] A. J. Collins, R. N. Foley, C. Herzog et al., "United States renal data system 2008 annual data report," *American Journal of Kidney Diseases*, vol. 53, supplement 1, pp. A6–A7, 2009.

[2] E. Stitt-Cavanagh, L. MacLeod, and C. Kennedy, "The podocyte in diabetic kidney disease," *The Scientific World Journal*, vol. 9, pp. 1127–1139, 2009.

[3] J. W. Leeuwis, T. Q. Nguyen, A. Dendooven, R. J. Kok, and R. Goldschmeding, "Targeting podocyte-associated diseases," *Advanced Drug Delivery Reviews*, vol. 62, no. 14, pp. 1325–1336, 2010.

[4] C. Faul, K. Asanuma, E. Yanagida-Asanuma, K. Kim, and P. Mundel, "Actin up: regulation of podocyte structure and function by components of the actin cytoskeleton," *Trends in Cell Biology*, vol. 17, no. 9, pp. 428–437, 2007.

[5] I. Shirato, T. Sakai, K. Kimura, Y. Tomino, and W. Kriz, "Cytoskeletal changes in podocytes associated with foot process effacement in Masugi nephritis," *American Journal of Pathology*, vol. 148, no. 4, pp. 1283–1296, 1996.

[6] M. Lachapelle and M. Bendayan, "Contractile proteins in podocytes: immunocytochemical localization of actin and alpha-actinin in normal and nephrotic rat kidneys," *Virchows Archiv*, vol. 60, no. 2, pp. 105–111, 1991.

[7] A. Togawa, J. Miyoshi, H. Ishizaki et al., "Progressive impairment of kidneys and reproductive organs in mice lacking Rho GDIα," *Oncogene*, vol. 18, no. 39, pp. 5373–5380, 1999.

[8] N. Kioka, K. Ueda, and T. Amachi, "Vinexin, CAP/ponsin, ArgBP2: a novel adaptor protein family regulating cytoskeletal organization and signal transduction," *Cell Structure and Function*, vol. 27, no. 1, pp. 1–7, 2002.

[9] G. Cestra, D. Toomre, S. Chang, and P. De Camilli, "The Abl/Arg substrate ArgBP2/nArgBP2 coordinates the function of multiple regulatory mechanisms converging on the actin cytoskeleton," *Proceedings of the National Academy of Sciences of the United States of America*, vol. 102, no. 5, pp. 1731–1736, 2005.

[10] K. Asanuma, E. Yanagida-Asanuma, M. Takagi, F. Kodama, and Y. Tomino, "The role of podocytes in proteinuria," *Nephrology*, vol. 12, supplement 3, pp. S15–S20, 2007.

[11] D. S. Courson and R. S. Rock, "Actin cross-link assembly and disassembly mechanics for α-actinin and fascin," *Journal of Biological Chemistry*, vol. 285, no. 34, pp. 26350–26357, 2010.

[12] H. Pavenstadt, W. Kriz, and M. Kretzler, "Cell biology of the glomerular podocyte," *Physiological Reviews*, vol. 83, no. 1, pp. 253–307, 2003.

[13] S. K. Akkina, Y. Zhang, G. L. Nelsestuen, W. S. Oetting, and H. N. Ibrahim, "Temporal stability of the urinary proteome after kidney transplant: more sensitive than protein composition?" *Journal of Proteome Research*, vol. 8, no. 1, pp. 94–103, 2009.

[14] N. L. Anderson and N. G. Anderson, "The human plasma proteome: history, character, and diagnostic prospects," *Molecular and Cellular Proteomics*, vol. 1, no. 11, pp. 845–867, 2002.

[15] K. Kawano, T. Hirashima, S. Mori, Y. Saitoh, M. Kurosumi, and T. Natori, "Spontaneous long-term hyperglycemic rat with diabetic complications: Otsuka Long-Evans Tokushima Fatty (OLETF) strain," *Diabetes*, vol. 41, no. 11, pp. 1422–1428, 1992.

[16] E. Ishimura, R. B. Sterzel, K. Budde, and M. Kashgarian, "Formation of extracellular matrix by cultured rat mesangial cells," *American Journal of Pathology*, vol. 134, no. 4, pp. 843–855, 1989.

[17] T. Ohse, J. W. Pippin, M. R. Vaughan, P. T. Brinkkoetter, R. D. Krofft, and S. J. Shankland, "Establishment of conditionally

immortalized mouse glomerular parietal epithelial cells in culture," *Journal of the American Society of Nephrology*, vol. 19, no. 10, pp. 1879–1890, 2008.

[18] H. Xu, L. Yang, W. Wang et al., "Antigen retrieval for proteomic characterization of formalin-fixed and paraffin-embedded tissues," *Journal of Proteome Research*, vol. 7, no. 3, pp. 1098–1108, 2008.

[19] A. Kakehashi, N. Ishii, T. Shibata et al., "Mitochondrial prohibitins and septin 9 are implicated in the onset of rat hepatocarcinogenesis," *Toxicological Sciences*, vol. 119, no. 1, pp. 61–72, 2011.

[20] A. Kinoshita, H. Wanibuchi, K. Morimura et al., "Phenobarbital at low dose exerts hormesis in rat hepatocarcinogenesis by reducing oxidative DNA damage, altering cell proliferation, apoptosis and gene expression," *Carcinogenesis*, vol. 24, no. 8, pp. 1389–1399, 2003.

[21] S. Esquenazi, H. E. P. Bazan, V. Bui, J. He, D. B. Kim, and N. G. Bazan, "Topical combination of NGF and DHA increases rabbit corneal nerve regeneration after photorefractive keratectomy," *Investigative Ophthalmology and Visual Science*, vol. 46, no. 9, pp. 3121–3127, 2005.

[22] T. Morioka, H. Koyama, H. Yamamura et al., "Role of H1-calponin in pancreatic AR42J cell differentiation into insulin-producing cells," *Diabetes*, vol. 52, no. 3, pp. 760–766, 2003.

[23] T. Turk, J. W. Leeuwis, J. Gray et al., "BMP signaling and podocyte markers are decreased in human diabetic nephropathy in association with CTGF overexpression," *Journal of Histochemistry and Cytochemistry*, vol. 57, no. 7, pp. 623–631, 2009.

[24] A. Kakehashi, M. Inoue, M. Wei, S. Fukushima, and H. Wanibuchi, "Cytokeratin 8/18 overexpression and complex formation as an indicator of GST-P positive foci transformation into hepatocellular carcinomas," *Toxicology and Applied Pharmacology*, vol. 238, no. 1, pp. 71–79, 2009.

[25] A. Kinoshita, H. Wanibuchi, K. Morimura et al., "Carcinogenicity of dimethylarsinic acid in Ogg1-deficient mice," *Cancer Science*, vol. 98, no. 6, pp. 803–814, 2007.

[26] D. Kobayashi, J. Kumagai, T. Morikawa et al., "An integrated approach of differential mass spectrometry and gene ontology analysis identified novel proteins regulating neuronal differentiation and survival," *Molecular and Cellular Proteomics*, vol. 8, no. 10, pp. 2350–2367, 2009.

[27] A. Pierce, R. D. Unwin, C. A. Evans et al., "Eight-channel iTRAQ enables comparison of the activity of six leukemogenic tyrosine kinases," *Molecular and Cellular Proteomics*, vol. 7, no. 5, pp. 853–863, 2008.

[28] B. Wang, E. A. Golemis, and G. D. Kruh, "ArgBP2, a multiple Src homology 3 domain-containing, Arg/Abl-interacting protein, is phosphorylated in v-Abl-transformed cells and localized in stress fibers and cardiocyte Z-disks," *Journal of Biological Chemistry*, vol. 272, no. 28, pp. 17542–17550, 1997.

[29] E. D. Goley, A. Rammohan, E. A. Znameroski, E. N. Firat-Karalar, D. Sept, and M. D. Welch, "An actin-filament-binding interface on the Arp2/3 complex is critical for nucleation and branch stability," *Proceedings of the National Academy of Sciences of the United States of America*, vol. 107, no. 18, pp. 8159–8164, 2010.

[30] M. Mosevitsky and I. Silicheva, "Subcellular and regional location of "brain" proteins BASP1 and MARCKS in kidney and testis," *Acta Histochemica*, vol. 113, no. 1, pp. 13–18, 2011.

[31] V. Delanote, J. Vandekerckhove, and J. Gettemans, "Plastins: versatile modulators of actin organization in (patho)physiological cellular processes," *Acta Pharmacologica Sinica*, vol. 26, no. 7, pp. 769–779, 2005.

[32] P. Niaudet, "Nephrotic syndrome in children," *Current Opinion in Pediatrics*, vol. 5, no. 2, pp. 174–179, 1993.

[33] M. A. Saleem, J. Zavadil, M. Bailly et al., "The molecular and functional phenotype of glomerular podocytes reveals key features of contractile smooth muscle cells," *American Journal of Physiology*, vol. 295, no. 4, pp. F959–F970, 2008.

[34] H. S. Choi, S. H. Yim, H. D. Xu et al., "Tropomyosin3 overexpression and a potential link to epithelial-mesenchymal transition in human hepatocellular carcinoma," *BMC Cancer*, vol. 10, article 122, 2010.

[35] C. A. Otey and O. Carpen, "α-actinin revisited: a fresh look at an old player," *Cell Motility and the Cytoskeleton*, vol. 58, no. 2, pp. 104–111, 2004.

[36] S. Bachmann, W. Kriz, C. Kuhn, and W. W. Franke, "Differentiation of cell types in the mammalian kidney by immunofluorescence microscopy using antibodies to intermediate filament proteins and desmoplakins," *Histochemistry*, vol. 77, no. 3, pp. 365–394, 1983.

[37] C. Dai, D. B. Stolz, S. I. Bastacky et al., "Essential role of integrin-linked kinase in podocyte biology: bridging the integrin and slit diaphragm signaling," *Journal of the American Society of Nephrology*, vol. 17, no. 8, pp. 2164–2175, 2006.

[38] Y. Zhang, J. Wada, I. Hashimoto et al., "Therapeutic approach for diabetic nephropathy using gene delivery of translocase of inner mitochondrial membrane 44 by reducing mitochondrial superoxide production," *Journal of the American Society of Nephrology*, vol. 17, no. 4, pp. 1090–1101, 2006.

NDT Advance Access published December 15, 2011

Nephrol Dial Transplant (2011) 0: 1–9
doi: 10.1093/ndt/gfr682

Original Article

Proteome analysis of laser microdissected glomeruli from formalin-fixed paraffin-embedded kidneys of autopsies of diabetic patients: nephronectin is associated with the development of diabetic glomerulosclerosis

Shinya Nakatani[1,2,3], Min Wei[1], Eiji Ishimura[2], Anna Kakehashi[1], Katsuhito Mori[3], Yoshiki Nishizawa[3], Masaaki Inaba[3] and Hideki Wanibuchi[1]

[1]Department of Pathology, Osaka City University Graduate School of Medicine, Osaka, Japan, [2]Department of Nephrology, Osaka City University Graduate School of Medicine, Osaka, Japan and [3]Department of Metabolism, Endocrinology and Molecular Medicine, Osaka City University Graduate School of Medicine, Osaka, Japan

Correspondence and offprint requests to: Eiji Ishimura; E-mail: ish@med.osaka-cu.ac.jp

Abstract

Background. To date, little proteomic information has been available from the glomeruli of diabetic patients, possibly due to the clinical limitations of renal biopsy in diabetic patients and insufficient quantities of such specimens for proteome analysis. The purpose of the present study was to identify altered protein expression profiles in diabetic glomeruli using formalin-fixed paraffin-embedded (FFPE) kidney tissues from diabetic patients.

Methods. Glomeruli were laser microdissected from FFPE autopsy kidney tissues from 10 patients with diabetic nephropathy and 10 non-diabetic control patients and underwent proteome analysis using QSTAR Elite liquid chromatography with tandem mass spectrometry and iTRAQ technology. Immunohistochemical analysis was performed on 93 autopsy samples from diabetic patients with and without nephropathy ($n = 45$ and $n = 48$, respectively).

Results. Thirty-one renal and urological disease-related proteins displayed a differential abundance in glomerular samples from patients with diabetic nephropathy compared with non-diabetic control patients. Among them, we found that nephronectin, which functions in the assembly of extracellular matrix, showed clearly positive immunoreactivity in diabetic glomeruli. The numerical fraction of nephronectin-positive glomerular cross sections was increased significantly in diabetic patients with nephropathy compared to those without nephropathy (32.1 ± 31.5 versus 4.14 ± 5.65%, $P < 0.0001$). Furthermore, there was a significant positive correlation between this numerical fraction of nephronectin-positive glomerular cross sections and the glomerular sclerosis index ($\rho = 0.881$, $P < 0.0001$, $n = 93$).

Conclusion. The present study demonstrated, for the first time, that nephronectin may be associated with the development of diabetic glomerulosclerosis and that proteome analysis with FFPE kidney tissues from diabetic patients with nephropathy is useful in understanding diabetic nephropathy.

Keywords: diabetic glomerulosclerosis; formalin-fixed paraffin-embedded tissues; nephronectin; proteome analysis

Introduction

Diabetic nephropathy is the most frequent cause of end-stage renal disease worldwide and currently accounts for ~40% of patients that require renal replacement therapy [1]. It is a renal disease that arises as a consequence of diabetes and affects ~30% of all such patients [2, 3]. The total number of people with diabetes is expected to increase from 171 million in 2000 to 366 million in 2030 [4]. Therefore, the number of people that develop diabetic nephropathy is also expected to increase. From this perspective, understanding the mechanisms and identification of novel biomarkers of diabetic nephropathy will be necessary to prevent the progression of diabetic nephropathy.

Recently, proteome analysis has increasingly been used in the discovery of disease-specific proteins and biomarkers of kidney diseases [5, 6]. Although proteome analysis of diabetic nephropathy has been performed using urine and serum specimens [7–11], it is not clear whether the proteins that are differentially expressed in these studies correlate directly with diabetic glomerular alterations or are useful as novel biomarkers. Thus, in order to investigate protein expression profiles that reflect diabetic glomeruli, a full proteomic analysis of diabetic glomeruli is essential. However, proteome analysis of glomeruli isolated from kidney biopsy specimens of diabetic patients is difficult due to the fact that renal biopsy specimens are clinically limited in diabetic patients and the quantities of glomeruli obtained from renal biopsy specimens are usually not sufficient for proteome analysis. Compared with renal biopsy specimens, we expect that sufficient amounts of glomerular tissue specimen could be isolated from formalin-fixed paraffin-embedded

(FFPE) autopsy kidney tissues for proteome analysis. Thus, research would be significantly advanced if FFPE kidney tissues of diabetic patients were made readily available for proteome analysis.

The purpose of the present study was to identify altered protein expression profiles in glomeruli from patients with diabetic nephropathy, using laser microdissected glomeruli from FFPE autopsy kidney tissues of diabetic patients with nephropathy and non-diabetic control patients, using QSTAR Elite liquid chromatography with tandem mass spectrometry (QSTAR Elite LC–MS/MS) and iTRAQ technology.

Materials and methods

Patients

Figure 1 indicates the workflow of this study. For the proteome analysis, 10 autopsy kidney specimens were obtained from diabetic patients with nephropathy, without hypertension or other renal disease, who did not undergo renal transplant, hemodialysis or peritoneal dialysis, during the period from December 2004 to December 2009 at Osaka City University Graduate School of Medicine. Ten control autopsy kidney specimens were obtained from age-matched non-diabetic patients without renal disease during the same period.

For immunohistochemical analysis, in addition to the above specimens, 83 autopsy kidney specimens from diabetic patients were obtained during the period from January 1997 to December 2009 at Osaka City University Graduate School of Medicine. A total of 93 diabetic kidneys comprised of 45 and 48 cases with and without nephropathy, respectively, were obtained. All autopsy kidney tissues used in the present study were fixed in 10% buffered formalin and embedded in paraffin blocks. Before paraffin embedding, all autopsy kidney specimens were fixed in formaldehyde for 3–7 days.

Clinical data [i.e. fasting plasma glucose, hemoglobinA1c (HbA1c), urea nitrogen, creatinine and estimated glomerular filtration rate (eGFR)] were assessed 1 month before death to accurately reflect the long-term condition of the patient, as described previously [12].

The Institutional Review Board at the Osaka City University Graduate School of Medicine approved the use of the autopsy specimens and clinical data in accordance with the Declaration of Helsinki and guidelines of the Osaka City University Graduate School of Medicine.

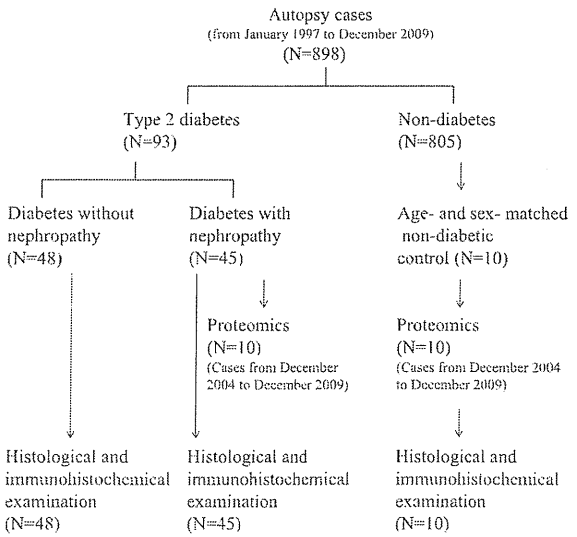

Fig. 1. Workflow of the study.

Collection of glomerular tissue specimen by laser microdissection

For each case, two 10-μm thick sections of FFPE kidney tissues that had been cut in 100-μm distance were placed on DIRECTOR™ slides (Expression Pathology, Gaithersburg, MD) for laser microdissection, deparaffinized and stained with hematoxylin. In each section, 20–25 fields of view (with three to eight glomerular cross sections per field) were randomly sampled at a magnification of ×100. The glomerular cross sections present in these fields were microdissected, using the Zeiss PALM® MB4 Microdissection System (Zeiss, Munich, Germany), according to the manufacturer's instruction, and collected into Adhesive Cap 500 clear tubes (Zeiss) containing 50 μL of liquid tissue buffer from the Liquid Tissue™ MS Protein Prep kit. Images of a representative FFPE section of an autopsy kidney before and after laser microdissection and the microdissected glomerular cross sections on the microcentrifuge tube cap are shown in Figure 2.

Based upon the results of our preliminary experiments, indicating that 1000 glomerular cross sections (5-μg protein) were necessary for proteome analysis, 100 glomerular cross sections were collected from two slides from each patient (50 glomerular cross sections per slide) by a random sampling method, and a total of 1000 glomerular cross sections from 10 diabetic patients with nephropathy were pooled. A total of 1000 glomerular cross sections from 10 non-diabetic patients without renal disease were pooled in a similar manner. The aim of the present study was to identify proteins that were commonly expressed in diabetic glomeruli and to compare them with those expressed in non-diabetic glomeruli. Since it was difficult to obtain sufficient amounts of glomeruli from individual diabetic patients with nephropathy or sufficient amounts of glomeruli from age- and sex-matched non-diabetic individual subjects and since multiple proteome analyses of each individual patient could therefore not be performed, we pooled the microdissected glomerular samples of 10 diabetic patients with nephropathy and of 10 non-diabetic patients, respectively.

Protein extraction, iTRAQ sample labeling and QSTAR Elite MS/MS analysis

Protein extraction was performed using the Liquid Tissue™ MS Protein Prep kit, according to the manufacturer's protocol. Briefly, aliquots of tissue buffer-containing microdissected glomerular cross sections were heated at 95°C for 90 min and digested with 1.5 μL of 1 μg/mL trypsin overnight at 37°C. After brief ultrasonication, insoluble material was removed from the cell lysates by centrifugation at 13 000 *g* for 15 min at 10°C. Protein concentrations were determined using the BCA Protein Assay kit (Pierce, IL). Protein reduction, alkylation, digestion and subsequent peptide labeling were performed using the AB Sciex iTRAQ Reagent Multi-Plex Kit (AB Sciex, Foster City, CA), according to the manufacturer's instructions with minor modifications [13, 14]. Briefly, 6 μg of protein from each sample was incubated at 60°C for 60 min in 20 μL of dissolution buffer and 2 μL of reducing reagent [50 mM tris-

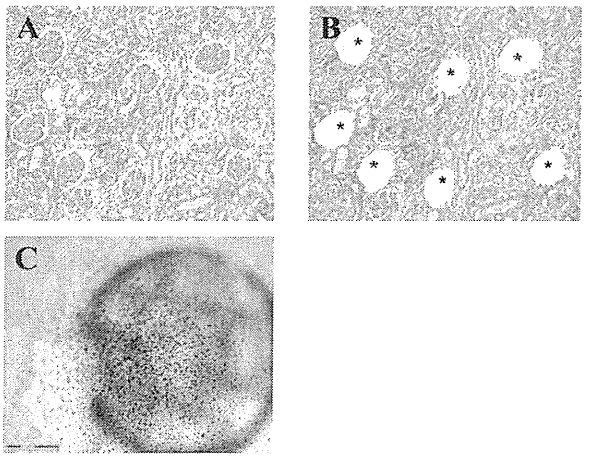

Fig. 2. FFPE section of an autopsy kidney: before microdissection (**A**); after microdissection (**B**), *indicates dissected glomerular cross sections; fragments of the microdissected glomeruli on the microcentrifuge tube cap (**C**).

(2-carboxyethyl) phosphine]. Free cysteine sulfhydryl groups were blocked by incubation with 1 μL of cysteine blocking reagent (20 mM methyl methanethiosulfonate) at room temperature for 10 min. Non-diabetic samples and diabetic nephropathy samples were labeled with iTRAQ114 and iTRAQ115, respectively, mixed in one tube and fractionated by six concentrations of KCl solutions (10, 50, 70, 100, 200 and 350 mM) using the ICAT cation exchange cartridge (AB Sciex). After desalting and concentrating, peptides of each fraction were quantified using a DiNa-AI nano LC System (KYA Technologies, Tokyo, Japan) coupled to the QSTAR Elite MS/MS through a NanoSpray ion source (AB Sciex, Concord, Canada), as described previously [14]. Protein Pilot 2.0 software (AB Sciex) with the Paragon™ Algorithm was used for the identification and relative quantification of proteins. Peptides were quantitated using the centroided reporter ion peak intensity. Intrasample channels were normalized, based on the median ratio for each channel across all proteins. Multiple isobaric tag samples were normalized by comparing the median protein ratios for the reference channel. Protein quantitative values were derived only from assigned peptides in both samples. Protein quantitative ratios statistics were calculated as the median of all peptide ratios [15, 16]. Statistically significant differences of protein expression were determined between the two groups using this software [14, 17], and protein ratios with P-values <0.05 were considered reliable [16, 18]. The tandem mass spectrometry data were searched against the human protein database from SwissProt 57.4 (20 257 sequences). Furthermore, information regarding the function, cellular location and correlation to disease of the identified proteins was obtained from Ingenuity Pathway Analysis (IPA; Ingenuity Systems, Mountain View, CA).

Nephronectin immunohistochemical analysis and evaluation of the numerical fraction of nephronectin-positive glomerular cross sections

Immunohistochemical staining was performed using the avidin-biotin immunoperoxidase method. Rabbit anti-human nephronectin antibody (Trans Genic Inc., Kumamoto, Japan) was used [1:100 dilution in phosphate-buffered saline (PBS)]. Briefly, after deparaffinization with xylene and gradual dehydration, antigen retrieval was undertaken with sodium citrate buffer at pH 6.0 in a microwave for 25 min and endogenous peroxidase activity was blocked by incubation with 3% hydrogen peroxide (H_2O_2) for 5 min. Sections were then incubated with 1.5% normal goat serum in PBS for 15 min and the first antibody was applied at 4°C overnight. A biotinylated goat anti-rabbit IgG was applied as a secondary antibody for 30 min and the avidin–biotin peroxidase complex was applied for 30 min. Rabbit serum IgG was applied as a negative control. The peroxidase reaction was developed using 0.02% 3,3-diaminobenzidine tetrahydrochloride and 0.03% hydrogen peroxide in Tris-buffered saline. Hematoxylin was used for counterstaining.

Glomeruli were defined as positive when positive staining of nephronectin was evident in >10% of the glomerular area. All glomeruli were counted in each specimen to calculate the numerical fraction of nephronectin-positive glomerular cross sections. Immunohistochemical analysis was carried out by two renal pathologists in a blinded manner.

Evaluation of glomerulosclerosis

FFPE kidney tissues were cut into 4-μm thick sections and stained with Periodic acid-Schiff. For evaluation of the glomerular sclerosis index, 20–25 fields of kidney sections (three to eight glomerular cross sections per field) were randomly selected at a magnification of ×100. The glomerular sclerosis index analysis was used to evaluate the degree of glomerulosclerosis [19, 20]. The severity of the lesions for each kidney was examined in 100 glomeruli using the random sampling method and graded from 0 to 4 points according to the proportion of morphological changes in each glomerulus (0, 0%; 1+, 1–25%; 2+, 26–50%; 3+, 51–75%; 4+, 76–100%). The number of glomeruli with lesions of grades 0, 1+, 2+, 3+ and 4+ was counted (n_0, n_1, n_2, n_3 and n_4, respectively). The glomerular sclerosis index was obtained according to the following formula: $(0 \times n_0 + 1 \times n_1 + 2 \times n_2 + 3 \times n_3 + 4 \times n_4)/100$ [20]. Histological examinations were carried out by two renal pathologists in a blinded manner.

Statistical analysis

Statistical analyses were performed using Graph-Pad Prism version 5.0 for Windows (Graphpad Software, San Diego, CA). Values are expressed as the mean ± SD. Normality of variance was tested by the *F*-test. Differences in the mean values of eGFR, urinary protein, fasting plasma glucose, HbA1c, creatinine, urea nitrogen and the numerical fraction of nephronectin-positive glomerular cross sections between groups were analyzed by Student's *t*-test when variance was normal and by Welch's *t*-test when variance was not. The glomerular sclerosis index was analyzed by Mann–Whitney test. The number of male and female diabetes patients with and without nephropathy was analyzed by chi-square test. The relationship between the numerical fraction of nephronectin-positive glomerular cross sections and the glomerular sclerosis index was assessed by non-parametric Spearman's rank correlation test. P-values <0.05 were considered significant.

Results

Clinical characteristics

The clinical characteristics of the diabetic patients with nephropathy ($n = 10$) and non-diabetic patients without renal disease ($n = 10$), whose kidney specimens were used for proteome analysis, are summarized in Table 1. The clinical characteristics of the diabetic patients with nephropathy were matched with non-diabetic patients, with respect to gender and age. Compared with non-diabetic patients, diabetic patients with nephropathy had significantly lower eGFR, significantly higher fasting plasma glucose and HbA1c levels ($P < 0.05$). The clinical characteristics of the 93 diabetic patients with and without nephropathy (including the 10 cases used in the above proteome analysis) in whom immunohistochemistry analyses were performed are summarized in Table 2. Compared with diabetic patients without nephropathy, those with nephropathy had significantly lower eGFR, significantly higher urea nitrogen, creatinine and urinary protein ($P < 0.05$). On the other hand, age, gender, fasting plasma glucose and HbA1c were not significantly different between the diabetic patients with and without nephropathy.

Proteome analysis

A total of 170 proteins were identified by iTRAQ labeling and QSTAR Elite LC–MS/MS system with 95% confidence. A total of 100 proteins displayed a significant differential abundance in glomerular samples of diabetic patients with nephropathy as compared to non-diabetic patients. They consisted of 55 and 45 proteins that were overexpressed (Table 3) and downexpressed (Table 4) in glomerular cross sections from diabetic patients with nephropathy. Among them, 20 overexpressed and 11 downexpressed proteins were related to renal and urological disease, based on the results of IPA. In the present study, we focused on nephronectin because it was overexpressed in glomeruli from diabetic patients with nephropathy and because nephronectin has been reported to function in the assembly of extracellular matrix and could play a crucial role in the development of the kidney [21, 22].

Analysis of glomerular nephronectin immunoreactivity

Consistent with a previous report [23], nephronectin immunoreactivity was found to be negative in normal glomeruli but positive in tubular epithelial cells of non-diabetic patients (Figure 3B). In contrast, nephronectin immunoreactivity was clearly positive in mesangial expansion, diffuse glomerular sclerosis (Figure 3D) and nodular glomerulosclerosis (Figure 3F) in diabetic patients. Nephronectin

Table 1. Clinical characteristics of 10 diabetic patients with nephropathy and 10 non-diabetic patients

Patient no.	Sex	Age	Cause of death	eGFR (mL/min/1.73m^2)	Fasting plasma glucose (mg/dL)	HbA1c (%)
Diabetic patients with nephropathy						
1	M	64	Cerebellar infarction	58.8	106	NA
2	M	41	Ischemic heart failure	81.9	485	NA
3	M	63	Acute cardiac infarction	44.3	NA	NA
4	M	57	Rectal cancer	49.8	343	7.2
5	M	75	Diffuse alveolar damage	66.3	412	8.4
6	M	75	Ischemic heart failure	29.5	400	8.4
7	M	62	Lung cancer	62.8	163	5.9
8	F	56	Ovarian cancer	56.0	286	NA
9	F	78	Terminal ileus	111.9	470	8.7
10	F	55	Meningitis	37.2	560	NA
Mean ± SD		63 ± 4		59.9 ± 7.5[a]	358 ± 150 (n = 9)[a]	8.7 ± 1.1 (n = 5)[a]
Non-diabetic patients						
11	M	66	Esophageal cancer	86.1	125	5.0
12	M	73	Gastric cancer	99.0	105	NA
13	M	43	Idiopathic portal hypertension	84.1	80	4.1
14	M	81	Lung cancer	86.6	83	5.6
15	M	70	Hard palate cancer	65.9	NA	NA
16	M	74	Lung cancer	100.5	93	5.1
17	M	67	Esophageal cancer	93.0	94	NA
18	F	52	Intestinal cancer	80.7	78	5.1
19	F	66	Ovarian cancer	63.6	92	NA
20	F	69	Cholangiocarcinoma	90.8	NA	NA
Mean ± SD		66 ± 3		85.0 ± 3.9	93.8 ± 15.4 (n = 8)	5.0 ± 0.5 (n = 5)

[a]The data are expressed as the mean ± SD. $P < 0.05$. NA, not available; HbA1c, hemoglobin A1c.

Table 2. Clinical characteristics of 93 Type 2 diabetic patients with and without nephropathy[a]

	Total (n = 93)	With nephropathy (n = 45)	Without nephropathy (n = 48)	P-values[b]
Age (years)	67.8 ± 8.8	66.9 ± 8.9	68.7 ± 8.8	0.34
Male/female	73/20	35/10	38/10	0.87
Fasting plasma glucose (mg/dL)	195 ± 78.1 (87)	205 ± 85.8 (41)	186 ± 70.0 (46)	0.26
HbA1c (%)	6.8 ± 1.6 (66)	7.0 ± 1.7 (30)	6.7 ± 1.5 (36)	0.47
Urea nitrogen (mg/dL)	32.6 ± 22.5	38.3 ± 24.3	27.2 ± 19.5	0.016
Creatinine (mg/dL)	1.6 ± 1.7	2.2 ± 2.1	1.1 ± 0.80	0.0027
eGFR (mL/min/1.73m^2)	60.4 ± 42.1	47.1 ± 35.7	73.0 ± 44.1	0.0026
Urinary protein (mg/dL)	41.0 ± 70.5 (73)	63.5 ± 81.7 (31)	23.3 ± 55.3 (42)	0.022

[a]The data are expressed as the mean ± SD. HbA1c, hemoglobin A1c. Clinical characteristics of some cases are not available as the clinical characteristics were not indicated in the autopsy records.
[b]Differences between diabetic patients with and without nephropathy.

immunoreactivity was positive in some exudative lesions, but was much less well stained (Figure 3H) compared with the mesangial expansion lesions. No staining was observed in negative control specimens (Figure 3I). In contrast, nephronectin immunoreactivity was positive in tubular epithelial cells of mouse kidney sections, which were used as positive controls (Figure 3J). In the present study, positive glomerular immunohistochemical staining of nephronectin was restricted to the extracellular matrix of the glomeruli. We could not clearly find intracellular staining either in mesangial cells, podocytes or endothelial cells (Figure 3D).

We further investigated nephronectin immunoreactivity in diabetic glomeruli in 93 diabetic patients, including those with and without nephropathy. As summarized in Table 5, the numerical fraction of nephronectin-positive glomerular cross sections was significantly higher in the kidneys from diabetic patients with and without nephropathy compared with those from non-diabetic patients (32.1 ± 31.5 versus 0.54 ± 0.36%, $P < 0.0001$ and 4.14 ± 5.65 versus 0.54 ± 0.36%, $P < 0.0001$, respectively). The numerical fraction of nephronectin-positive glomerular cross sections in the kidneys from diabetic patients with nephropathy was significantly higher than in those without nephropathy (32.1 ± 31.5 versus 4.14 ± 5.65%, respectively, $P < 0.0001$).

Correlation analysis of the numerical fraction of nephronectin-positive glomerular cross sections and glomerulosclerosis

The results of the histological glomerular sclerosis index in 93 diabetic patients with and without nephropathy and 10 non-diabetic patients are shown in Table 5. The glomerular sclerosis index in the kidneys from diabetic patients with nephropathy was significantly higher compared with that of the non-diabetic patients (1.51 ± 1.01 versus 0.25 ± 0.17,

Table 3. Significantly overexpressed proteins in specimen of microdissected glomerular cross sections from diabetic patients with diabetic nephropathy and their cellular locations

Protein name	GI number	Fold change Versus non-diabetic glomeruli	P-value	Location
Renal and urological disease-related proteins				
Clusterin	116533	2.42	0.0001	Extracellular space
Complement factor H	158517847	1.96	0.0002	Extracellular space
Amyloid P component, serum	730704	1.83	0.0001	Extracellular space
Complement component 3	119370332	1.76	0.0001	Extracellular space
Collagen, Type VI, alpha 1	125987811	1.70	0.0001	Extracellular space
Apolipoprotein E	114039	1.68	0.01	Extracellular space
Transglutaminase 2	20141877	1.58	0.0007	Cytoplasm
Complement component 4A	81175238	1.57	0.0102	Extracellular space
Serpin peptidase inhibitor, clade A	112874	1.49	0.0001	Extracellular space
Transthyretin	136464	1.47	0.0131	Extracellular space
Integrin, alpha 1	124056463	1.43	0.037	Plasma membrane
Fibronectin 1	2506872	1.43	0.0001	Plasma membrane
Fatty acid-binding protein 1, liver	119808	1.37	0.032	Cytoplasm
Nephronectin	**158563963**	**1.25**	**0.0006**	**Extracellular space**
Collagen, Type IV, alpha 4	259016360	1.24	0.0001	Extracellular space
Laminin, beta 2	156630892	1.23	0.0001	Extracellular space
Collagen, Type IV, alpha 3	134035067	1.21	0.0001	Extracellular space
Caldesmon 1	2498204	1.19	0.0089	Cytoplasm
Serpin peptidase inhibitor, clade C member 1	113936	1.19	0.0046	Extracellular space
Collagen, Type IV, alpha 5	461675	1.166	0.01	Extracellular space
Other proteins				
Complement component 9	1352108	2.83	0.0001	Extracellular space
Keratin 9	239938886	2.55	0.0001	Cytoplasm
Alpha-1-microglobulin/bikunin precursor	122801	2.44	0.0001	Extracellular space
Vitronectin	139653	2.13	0.0001	Extracellular space
Fibrillin 1	251757263	1.89	0.0001	Extracellular space
Collagen, Type VI, alpha 2	125987812	1.86	0.0001	Extracellular space
Collagen, Type IV, alpha 1	125987809	1.75	0.0001	Extracellular space
Collagen, Type VI, alpha 3	215274244	1.73	0.0001	Extracellular space
Collagen, Type IV, alpha 2	143811377	1.67	0.0001	Extracellular space
Immunoglobulin heavy constant alpha 1	113584	1.67	0.0028	Extracellular space
Complement component 4-binding protein, alpha	416733	1.67	0.010	Extracellular space
Immunoglobulin kappa constant	125145	1.65	0.0001	Extracellular space
Keratin 1	238054406	1.59	0.0001	Cytoplasm
Alcohol dehydrogenase 1 beta polypeptide	113394	1.45	0.0012	Cytoplasm
Keratin 2	239938650	1.40	0.0001	Cytoplasm
Ferritin, light polypeptide	120523	1.38	0.0034	Cytoplasm
Immunoglobulin heavy constant gamma 2	218512079	1.38	0.0001	Plasma membrane
Heparan sulfate proteoglycan 2	218512120	1.36	0.0001	Plasma membrane
Laminin, gamma 1	224471885	1.31	0.0001	Extracellular space
Serpin peptidase inhibitor	1703025	1.29	0.0001	Extracellular space
Orosomucoid-1	112877	1.26	0.0053	Extracellular space
Nidogen 1	251757450	1.25	0.0001	Extracellular space
Collagen, Type XVIII, alpha 1	215274264	1.23	0.0001	Extracellular space
Laminin, alpha 5	229463053	1.23	0.0001	Extracellular space
Vinculin	21903479	1.18	0.0001	Plasma membrane
Keratin 10	269849769	1.67	0.0001	Cytoplasm
Filamin A, alpha	116241365	1.14	0.0001	Cytoplasm
Transgelin 2	586000	1.13	0.0019	Cytoplasm
Glyceraldehyde-3-phosphate dehydrogenase	120649	1.12	0.0092	Cytoplasm
Betaine—homocysteine S-methyltransferase	145559446	1.12	0.0031	Cytoplasm
Fibrinogen beta chain	399492	1.10	0.0289	Extracellular space
Thymosin-like 3	189035974	1.10	0.0026	Unknown
Pyruvate kinase, muscle	20178296	1.09	0.037	Cytoplasm
S100 calcium-binding protein A9	115444	1.08	0.0147	Cytoplasm
Talin 1	81175200	1.06	0.0384	Plasma membrane

$P < 0.0001$, respectively). The glomerular sclerosis index in the kidneys from diabetic patients with nephropathy was significantly higher than in those without nephropathy (1.51 ± 1.01 versus 0.44 ± 0.35, $P < 0.0001$, respectively). There were no significant differences in the glomerular sclerosis index between diabetic patients without nephropathy and non-diabetic patients (0.44 ± 0.35 versus 0.25 ± 0.17, $P = 0.073$, respectively).

The relationship between the numerical fraction of nephronectin-positive glomerular cross sections and the glomerular sclerosis index in diabetic patients is shown in Figure 4. There was a significant positive correlation